

THE INFLUENCE OF WATER SORPTION ON  
THE DYNAMIC MECHANICAL PROPERTIES OF NYLON 6-6  
AND THE PLASTICISING EFFECT OF WATER

by

JACQUES MARIE RAYMOND QUISTWATER

B. A., University of British Columbia, 1954

A THESIS SUBMITTED IN PARTIAL FULFILMENT OF  
THE REQUIREMENTS FOR THE DEGREE OF

Master of Science

in the Department

of

CHEMISTRY

We accept this thesis as conforming to the  
required standard

THE UNIVERSITY OF BRITISH COLUMBIA

April, 1958

# ABSTRACT

Much work has recently been done on studies of mechanical and electrical dispersion phenomena in polymers. Many workers have been active studying the effect of plasticisers, irradiation, heat, and mechanical treatment, copolymerisation, and cross-linking, such as vulcanisation, on a large number of high polymers. In spite of its great technological importance, the effect of humidity on the mechanical properties of textile fibres has not been studied in a systematic way. The present investigation is an attempt at studying the influence of humidity on the modulus and energy dissipation of nylon 6-6 monofilaments.

The modulus and energy loss were determined using a low-frequency vibrometer, over the full range of relative humidities at 9, 35, and 60 °C., using 15 denier nylon monofilaments. Values of these empirical quantities were plotted as functions of frequency and humidity, and water content. The results were discussed taking into account the fact that water sorbed by fibres is present predominantly in the amorphous regions, and might be expected to break hydrogen bonds existing between adjacent peptide links, thereby reducing molecular interaction, and facilitating segmental motion. A mechanism was proposed in order to explain the results. The values of the tangent of the loss angle were compared with recent work by Sauer et al.

Using expressions derived by Ferry and coworkers, apparent activation energies for the flow processes were calculated at a number of fixed water contents, and were found to vary between 26.3 and 110 kcal./mole.

In presenting this thesis in partial fulfilment of the requirements for an advanced degree at the University of British Columbia, I agree that the Library shall make it freely available for reference and study. I further agree that permission for extensive copying of this thesis for scholarly purposes may be granted by the Head of my Department or by his representative. It is understood that copying or publication of this thesis for financial gain shall not be allowed without my written permission.

Department of Chemistry

The University of British Columbia,  
Vancouver 8, Canada.

Date May 1, 1958.

## TABLE OF CONTENTS

I. Theoretical and Experimental Introduction. . . . .	p. 1.
A. Historical Survey. . . . .	p. 1
B. Recent Work on the Mechanical Properties of Polymers. p.	1
1. Types of Experiments . . . . .	p. 1
a. Experiments in which Stress, Strain, or Modulus is Studied as a Function of Time or Frequency . p.	2
b. Stress-Strain Experiments . . . . .	p. 4
c. Experiments in which Modulus and Energy Loss are studied as Functions of Temperature . . . . p.	4
2. Correlation of Time and Temperature Effects . . . .	p. 6
3. Influence of Humidity, Copolymerisation, and Irra- diation. . . . .	p. 7
C. Dielectric Studies on High Polymers . . . . .	p. 9
D. Correlation between Mechanical and Dielectric "isper- sions in Polymers.. . . .	p. 10
E. Experimental Methods. . . . .	p. 11
II. Apparatus and Experiments. . . . .	p. 14
A. Description of the Apparatus. . . . .	p. 14
B. Calibration of the Solenoids and Determination of Parameters. . . . .	p. 21
III. Results. . . . .	p. 26
IV. Discussion.. . . .	p. 31
V. Appendix . . . . .	p. 39
VI. Bibliography . . . . .	p. 42

## THEORETICAL AND EXPERIMENTAL INTRODUCTION

### A. Historical Survey

Studies of dynamic modulus, energy loss, and stress relaxation, and creep have been performed on a variety of materials, including wood, rubber, metals, and natural and synthetic fibres. These studies were initiated by Hooke who enunciated the law of elasticity bearing his name. As a result of studies on the extension of metals under various loads, Young defined a tensile modulus  $E' = (F/A) / (\Delta l/l)$ , where  $F$  is the force on a cross-sectional area  $A$ , and  $\Delta l$  is the elongation of a length  $l$ . The studies of viscoelasticity were greatly extended by Voigt and Maxwell, who postulated various mechanical analogies, consisting of arrangements of springs and dashpots, to explain the observed viscoelastic behaviour<sup>1</sup>. The theoretical aspects were extended again by Eyring's application of his theory of rate processes, leading to a non-Newtonian viscosity<sup>2</sup>, and by the concept of a distribution of relaxation and retardation times, as advanced by Tobolsky<sup>3</sup>, Kuhn<sup>4</sup>, Becker<sup>5</sup>, and Ferry and co-workers<sup>6</sup>. A large number of workers have investigated the mechanical properties of polymers using various techniques, which will be elaborated in subsequent paragraphs.

### B. Recent Work on the Mechanical Properties of High Polymers.

#### 1. Types of experiments.

Basically, three types of experiments can be performed. The first type, that in which stress, strain, or modulus

is studied as a function of time or frequency, has been investigated most extensively. Experiments that fall in this class include stress relaxation, creep experiments, vibrational, torsional studies, and sound propagation. The second type of experiments, in which stress is studied as a function of strain, is a much smaller group. The third type of experiment involves studies of modulus as a function of temperature. A number of workers have carried out a large number of investigations in this field, reporting results that show the following general trends: below the glass temperature, the modulus decreases slowly with increasing temperature, near the glass temperature, the modulus decreases rapidly with increasing temperature, whereas above the glass temperature, in the region of rubber-like elasticity, the modulus increases with increasing temperature. Corresponding to each sharp modulus decrease in a transition temperature range, there is a maximum in energy dissipation in vibrational experiments.

a. Experiments in which Stress, Strain, or Modulus is studied as a Function of Time or Frequency.

<sup>7</sup>  
Ferry initiated comprehensive studies on the  
<sup>8</sup>  
rheology of polymer solutions; Ledderman studied the creep  
<sup>9</sup> <sup>10</sup> <sup>11</sup>  
behaviour of various fibres. Harris, Speakman, and Meredith,  
examined the stress-strain properties of wool and other fibres.  
<sup>3,12</sup>  
Tobolsky and associates have made extensive studies of rubber,  
polyethylene, polytetrafluoroethylene, methacrylates, and urethanes  
<sup>13</sup> <sup>14</sup> <sup>15</sup>  
by stress relaxation. Nolle, Ferry, and Guth have investigated

high-frequency vibrational properties of rubbers. Ballou<sup>20</sup> and Smith<sup>21</sup> and Fujino and coworkers<sup>22</sup> have studied the vibrational properties over a wide frequency range. Hamburger has attempted to correlate sonic techniques and stress-strain tests at normal speed on filaments and yarns. More recently, Hammerle and Montgomery<sup>23</sup>, working with nylon<sup>6-6</sup>, have verified the fact that the shear modulus and energy loss can be predicted from the relaxation of torque, as predicted by Alfrey.

Ferry and coworkers<sup>24</sup> have carried out wide investigations on rheological properties of polymer solutions, and, more recently, on solid polymers such as polystyrene, polyvinyl acetate, various methacrylates, and others. By reducing results obtained at a number of temperatures to one arbitrarily chosen temperature, they have succeeded in superimposing all results for any one polymer onto one master curve. They have calculated activation energies for viscous flow from the graphs of the temperature reduction factor against temperature. Ferry, Grandine, and Fitzgerald<sup>6,24</sup> have derived methods of obtaining the distribution functions of relaxation and retardation times for rubber-like polymers including polystyrene, polyisobutylene, and various methacrylates.

Fujino and coworkers<sup>21</sup> have studied the properties of rayons, silks, and nylon 6 over a very wide frequency range, at 20°C. and 65% relative humidity. Applying the method of Ferry to calculate the distribution functions, they found them to be, in almost all cases, between  $10^9$  and  $10^{10}$  dynes / cm<sup>2</sup>, within

the time-scale  $10^0 - 10^{-7}$  sec. They also investigated the effect of crystallisation and molecular orientation upon the relaxation spectra of terylene, nylon 6, polyvinyl chloride, and polyvinyl alcohol, using some physical treatments, such as heat treatment and cold drawing.

b. Stress-Strain Experiments.

In this type of experiment, the stress developed by a given extension in a constant rate of load or constant rate of elongation experiment is determined. Fibrous materials display histeretic behaviour in loading-unloading cycles. It has been found that the stress is dependent not only on the strain, but also on the rate of strain, and also, as would be expected, on temperature and humidity as well.

<sup>2,26</sup>  
Halsey and Eyring applied the theory of rate processes to these phenomena, and derived the hyperbolic sine law of viscous flow. By using this law, they were able to interpret visco-elastic experiments with only one, two, or three relaxation mechanisms, rather than with an infinite (or at least a very large) number of relaxation times required if Newtonian viscosity is presupposed. In addition to applying it to stress-strain experiments, they also applied this law to the creep data obtained by Leaderman<sup>8</sup> for viscose, cellulose acetate, and silk, and obtained good fits. They calculated free energies of activation of the order of 25 kilocalories per mole for these materials.

c. Experiments in which Modulus and Energy Loss are studied as Functions of Temperature.



13

Nolle has studied the mechanical properties of synthetic and natural rubber, both unvulcanised and vulcanised, over a wide frequency and temperature range. In addition, he performed some experiments on the effect of added carbon black, as a "filler", on the properties of the rubbers. It has been postulated that the carbon black exists in the rubber as a separate phase, and may therefore be expected to exert a marked effect on the dynamic properties of the rubber. His experiments have, in fact, confirmed this view.

27

Sauer, Kline, and others have examined the dynamic properties of both crystalline and non-crystalline polymers. They report that polyethylene and polytetrafluoroethylene, both crystalline materials, exhibit maxima in the energy loss versus temperature curve, at temperatures well below room temperature. On the other hand, polystyrene, which is amorphous, does not exhibit any maxima. One should, however, not generalise from these observations, for energy loss maxima have been observed at temperatures well below room temperature for various methacrylates, which are amorphous. They have also examined the effect of branching on the mechanical properties of polyethylene. In addition, they

28

have also investigated the effect of irradiation on the dynamic properties of nylon 6-6, nylon 6-10, and a copolymer of nylon 6-6, nylon 6-10, and nylon 6, as well as the effect of humidity on

29, 30

the value and temperature of the energy loss maximum for nylon 6-6, in a very qualitative fashion. Fitzgerald has studied the

29

31

mechanical resonance dispersion in teflon, and reports a satisfactory

agreement between experimental results and the behaviour predicted from the simple mechanical model he postulates. He obtains an activation energy of 13.2 kcal./mole.

In addition, Wolf and his school<sup>32</sup> have examined the influence of temperature on the dynamic tensile modulus and energy loss for a large number of polymers, both crystalline and non-crystalline. Price and Dunell<sup>33</sup> have reported the modulus and loss factor for viscose rayon within the temperature range 0 to - 80 C. A number of workers at the Imperial Chemical Industries laboratories in Great Britain have studied the modulus and energy loss factor of various acrylic polymers, and polyethylene over a temperature range of about 43,44,45<sup>o</sup> 300 C.

## 2. Correlation of Time and Temperature Effects.

The time-temperature superposition principle has been applied by workers such as Tobolsky<sup>3</sup> and Ferry<sup>6</sup>. Ferry has investigated a large number of acrylic polymers, and has been successful in superposing results obtained at various temperatures on one master curve, at an arbitrarily chosen temperature. Generally speaking, the time-temperature superposition principle can be applied to amorphous polymers. Very little information on its application to semicrystalline polymers is presently available.

Dunell<sup>17</sup> correlated stress relaxation and vibrational properties for a number of rubbers and textile fibres, and reported an order of magnitude agreement between observed values

of the dynamic energy loss and values calculated from Becker's distribution function. In most cases, it was found that the losses predicted from stress relaxation data are smaller than the observed dynamic losses. F. M. Bueche<sup>39</sup> has investigated and discussed the Young's modulus of semicrystalline substances and the mechanical properties of various rubbers. Making certain assumptions, he derives an equation for Young's modulus, for semicrystalline polymers, and reports quite good agreement between values of the modulus obtained from it, and empirical values, for polyethylene, but not for natural rubber.

Yoshitomi et al.<sup>35</sup> have investigated the stress relaxation of polycaproamide (Nylon 6) of low crystallinity. They applied Ferry's reduction method to reduce the results at 0 and 75% relative humidity at a number of temperatures to respective master curves. These two curves were further reduced to one curve by taking into account a molecular theory of crystalline polymers. Using a first order approximation method, they obtained the relaxation spectrum over a very wide time scale range -- 10<sup>21</sup> sec, in good agreement with the more limited data obtained by Fujino<sup>21</sup> and by Tokita.<sup>36</sup>

### 3. Influence of Humidity, Copolymerisation, and Irradiation.

Meyer and Lotmar<sup>38</sup> have examined qualitatively the effect of moisture content on the dynamic Young's modulus of a number of rayons, and on ramie and hemp. For all fibres, they reported a very considerable decrease in the modulus as the moisture content was increased, Anderson reported similar results for viscose rayon, in the frequency range 25 - 40 c.p.s. de Vries reported

a decrease in dynamic modulus, determined at 9 kc./s, with increasing moisture content, which amounted to about 4.3% decrease in modulus per 1% increase in moisture regain over the range 40 to 85% relative humidity, for Fortisan.<sup>38</sup>

In very recent publications, Tokita<sup>39</sup> and Kanamaru discuss the viscoelasticity of viscose and acetate rayons crosslinked to various degrees by tetramethylene bisethylene urea and tetramethylene-diisocyanate urea. They report that, as crosslinking increases, a minimum in the modulus and the apparent activation energy occurs, the lowest values being  $9 \times 10^{10}$  dynes / cm.<sup>2</sup>, and 95 kcal./mole respectively. They report a strong relative humidity dependence of these values, attributable to a solvating, or plasticising effect of water.

In this laboratory, Price, Pattison,<sup>37</sup> McIntyre and Dunell have carried out rather limited studies on the effect of temperature and humidity changes on the dynamic mechanical properties of nylon 6-6, viscose, and acetate rayon, and polyethylene. The polyethylene, as might be expected, was found to be quite insensitive to humidity changes. The properties of the other materials, however, were found to be strongly influenced by humidity changes.

Woodward, Sauer, Deeley and Kline have studied the change of modulus and energy loss versus temperature for a copolymer of nylon 6, 6-6, and 6-10, over a wide temperature range, from about 80 to 430<sup>o</sup> K.<sup>29</sup> They have also examined the effect of

irradiation on the dynamic mechanical properties of nylon 6-6<sup>27,29</sup> and polyethylene. The predominant effect of neutron and gamma irradiation appears to be that of introducing cross-linking<sup>30</sup> and destroying crystallinity.

### C. Dielectric Studies on High Polymers.

<sup>40</sup>  
Fuoss has carried out very extensive investigations on the electrical properties of a number of polymers, but primarily on polyvinyl chloride. He found that the electrical properties of polyvinyl-chloride depend on its thermal history -- as a result of pyrolysis, which leads to formation of hydrogen chloride, which is released very slowly within the polymer. The dielectric constant changes with time in a way which suggests a relaxation mechanism. Examining the system polyvinyl chloride-tri-cresyl phosphate at 40 °C., and 20 to 10<sup>4</sup> c.p.s., and a variety of compositions, he observed maximum change in the electrical properties in the range 50-70% polyvinyl chloride, and postulated a hindrance of freedom of orientation of dipoles in polymeric materials in applied electric fields. He also investigated the effect of a large number of plasticisers, and found that the dielectric constant and the dielectric loss factor were dependent upon the size and strength of the polar groups of both the polymers and the plasticisers, and the flexibility of the bond of the polar group to the polymer chain. He also observed that in the system polyvinyl chloride-20% diphenyl, the electrical properties are most markedly affected in the low concentration (0 to 2%) range of compositions, and concluded that this represented a viscosity phenomenon. He

discussed these dipole moments on a theoretical basis, and showed that the results for the polyvinyl chloride-diphenyl system were in agreement with theoretical deductions.

41

Davies, Miller and Busse carried out investigations parallel to Fuoss', on polyvinyl chloride plasticised with dimethylthianthrene, tritolyl phosphate, and dioctyl phthalate. They also separated the dielectric loss into a loss due to dipole rotation and a loss due to ionic conduction. Observing that the apparent energy of activation for mechanical deformation and dipole rotation are of about the same magnitude for these various plastics, they suggest that the chain units that move in mechanical deformations are of the same order of magnitude as the size of the chain units that move with dipole rotations.

#### D. Correlation Between Mechanical and Dielectric Dispersions in Polymers.

32,42

Several papers published in Kolloid Zeitschrift point out the parallelism between mechanical dispersion and dielectric relaxation phenomena in high polymers.

42

Heyboer reports observing two peaks in both the mechanical and the electrical energy loss versus temperature curves for polymethyl methacrylate. The high temperature mechanical energy loss maximum corresponds to an activation energy of approximately 100 kcal./mole; the low temperature one, to approximately 18 kcal./mole. The magnitudes of the loss peaks for dielectric relaxation exhibit the

reverse behaviour, with the high temperature peak being the smaller. Examining the structure of methacrylate polymers, he ascribes the high temperature transitions, with large relaxation time, to the motion of the paraffin-backbone of the polymer, and the low temperature transition, with small relaxation time, to motions of the strongly polar methacrylate part of the polymer.

A series of papers published by workers at Imperial Chemical Industries laboratories in Great Britain discussed the relation between the structure of polymers and their dynamic mechanical and electrical properties. They report activation energies varying from about 20 to 130 kcal./mole for polymethyl methacrylate and polymethyl  $\alpha$ -chloroacrylate, depending on the method used to evaluate them.<sup>43</sup> They examined the mechanical properties of a large number of methacrylates over a temperature range of - 200 to about 130°C, and reported activation energies for low-temperature processes between 3 and 11 kcal./mole.<sup>44</sup> Oakes and Robinson<sup>45</sup> report the dynamic mechanical and electrical properties of polyethylene over a wide temperature range, and report peaks in the mechanical energy dissipation factor at about -100, 0 and 60°C, for which they calculate activation energies of 6, 30 and 40 kcal./mole respectively.

#### E. Experimental Methods.

Various methods are available for studying the mechanical properties of high polymers, enabling one to choose between experiments on single filaments, on yarns, on films,

or on rods or blocks of the polymers. The most common types of mechanical experiments performed on fibres, however, are creep extensions, stress relaxation, vibrational, and torsional experiments. Methods involving sound propagation through rods of the polymer are similar to vibrational experiments inasmuch as both involve the application of strains of very short duration. Most experimental methods depend upon one or more of the following conditions: constant strain, constant stress, constant rate of strain, constant rate of stress, or sinusoidal variation of stress and strain. Such experiments therefore give information concerning stress-strain-time behaviour. Vibrational experiments enable this study to be extended over strains of very short duration, and provide a set of data which complements results obtainable from other experiments, such as creep and stress-strain studies, for which the time base is much longer.

Two types of vibrational experiments can be made - one in which a mass is attached to the fibre and the free vibrations of the system are measured, and the other in which the fibre is subjected to forced vibrations by applying a displacement varying sinusoidally with time. The resonant frequency of the system can be altered by changing either the length of the vibrating filament, or the mass of the transducer. As mentioned previously, a third method consists in propagating a sound wave through the polymer sample, and measuring its velocity and attenuation.

In most vibration experiments, the



strain amplitude is kept small, so that the stress may be treated as linearly related to the strain, and linear differential equations relating stress, strain, and time may be used. The periodic strain resulting from the sinusoidal stress is generally out of phase with the stress, and is described by an expression of the form  $a = a_0 \sin(2\pi ft - \theta)$  where  $\theta$  is the phase angle between the stress and the strain. The strain can also be thought of as consisting of two components, one of which is in phase with the applied stress, and the other of which is  $90^\circ$  out of phase with the applied stress. The stress divided by the component of the strain in phase with the stress is termed the energy loss  $E''$ . This relationship may conveniently be described by the complex dynamic modulus:

$$E^* = E' + iE'' = E' + i\eta\omega \quad (1)$$

where  $E^*$  is the complex dynamic modulus,  $E'$  is a measure of the elastic energy stored and recovered during each cycle of deformation, (the Hookean part of the viscoelastic behaviour) and  $E''$  is proportional to the energy dissipated during each cycle, (resulting from those elements of the structure that do not respond instantaneously to a given deformation)  $E''$  can be equated to  $\eta\omega$  in which  $\eta$  represents the resultant viscosity of a set of Newtonian dashpots giving rise to the energy dissipation. Characterisation of the dynamic mechanical properties of any material then requires the evaluation of both  $E'$  and  $E''$  as functions of frequency, temperature, and moisture content. As in most cases one is dealing with a set of viscosities or relaxation times, the resultant viscosity will be frequency dependent.

## APPARATUS AND EXPERIMENTS

The dynamic Young's modulus  $E'$  and the energy loss factor  $E''$  for 15 denier nylon monofilaments were determined at various conditions of temperature and humidity, using a technique similar to that of Dunell and Dillon.<sup>17</sup> The latter apparatus was very similar to that of Lyons and Prettyman<sup>19</sup> and also to the Firestone resonance vibrator for rubber samples in shear,<sup>16</sup> as described by Dillon, Prettyman and Hall.

### Descriptions of the Apparatus.

The apparatus used is sketched schematically in Figures 1 to 3. The driving mechanism consists of a solenoid of fine wire W wound on a paper core C which is cemented to a disc and a spindle D constructed from aluminum tubing, the solenoid coil lying in a radial magnetic field which traverses the annular space E in the magnetic circuit shown in Figure 3. The unit is suspended at each end by nylon filaments F which can be lengthened or shortened and moved back and forth at right angles to the axis of the vibrator unit to centre it in the magnetic field and insure that there is no contact between the coil and the sides of the angular gap in which it is located.

The permanent magnetic field is maintained by the two powerful permanent magnets N of Figure 2, two similar poles N, N, facing one another on one side of the radial gap, and a cylinder S forming the opposite pole on the other side of the gap. The filaments G which are to be tested are each cemented at one end to small thin pieces of aluminum each of which is in turn inserted

into a slot at each end of the shaft of the vibrator unit and made fast there with a small pin H. The other end of the filaments pass, through a relative humidity and temperature adjusting boxes J, to pulleys K at the end of the apparatus, and are tensioned by the weights L. The filaments may be clamped at various positions by screwing together fixed clamps, operable from without the chambers.

The transducer assemblies used in these experiments consisted of three solenoid coils wound coaxially on a horizontal spindle and lying in a radial magnetic field. The solenoid coils consisted respectively of about 2, 25, and 90 turns of no. 40 copper magnet wire. These three coils were so wound in order that one could always obtain a reading somewhere on the scale of a Leeds and Northrup thermomilliammeter whose full scale reading could be adjusted to 2, 10, or 50 milliamperes. The frequency of vibration of the transducer assembly could be changed continuously by altering the frequency of the applied electromotive force, which is, in fact, the frequency of vibration. The apparatus could be tuned to mechanical resonance by adjusting the frequency of the Hewlett-Packard low frequency oscillator used. The exact resonant frequency could be determined by determining the frequency at which the amplitude of vibration was a maximum for a given current value, or, for frequencies in excess of 10, c.p.s., by that frequency at which the peak to peak amplitude of the voltage across the solenoid coil was a maximum as displayed on an oscilloscope. The latter method was used as much as possible, inasmuch as stray mechanical vibrations of the system as a whole seemed to have a less pronounced effect.

As neither high humidities nor very low humidities could be readily achieved within the constant temperature room available, it was decided to enclose the fibres within constant humidity chambers, using the constant temperature room in order to control the temperature at  $35^{\circ}\text{C}$ . within plus or minus  $0.1$  to  $0.3^{\circ}\text{C}$ . The chambers were constructed of lucite and were provided with clamps operable from without the boxes, located at 5, 10, 15, 30, and 60 cm. from the end nearest the transducer assembly. Provision was also made for measuring the relative humidity at eight points within the boxes, using wet and dry junction thermocouples <sup>46</sup>. Air of controlled relative humidity was admitted within the chambers by means of an air manifold running the length of the boxes, the air being introduced into the manifold at the centre of the box. During the course of the experiments, the humidity within the boxes was checked periodically, and was found to be reasonably homogeneous - in all cases, the variation did not exceed 2%. Later, the average humidity of the air was measured by passing it over Aminco-Dunmore Electric Hydrometer wide range humidity sensing elements. The elements were coupled to a Bristol recorder, and the humidity reported for any particular experiment is the average obtained from the recorder trace.

The humidity of the air was adjusted by splitting the stream of compressed air, and passing one portion of it through drying towers of silica gel, and the other, through gas dispersion tubes into vessels filled with water, and immersed in an oil-filled constant temperature bath controlled by a Zeitfuchs-Doty thermoregulator to plus or minus  $0.01^{\circ}\text{C}$ . at  $35^{\circ}\text{C}$ . The two streams of air were then re-

combined, and passed over the humidity sensing unit, just before entering the lucite boxes enclosing the test filaments. The relative humidity of the air could be altered to practically any desired value by adjusting the volume of air passing through the drying columns and saturating vessels. When no air was passed through the saturating vessels, a low relative humidity of 11% could be achieved, using freshly regenerated silica gel: when the entire stream was passed through the saturating vessels, a maximum relative humidity of 96% could be obtained.

Essentially the same experimental set-up was used to determine the mechanical properties at 9<sup>°</sup>C., with the following modifications. In order to condense out as much water as possible, the compressed air stream was passed through cooling coils located immediately in front of the cooling fan used to cool the room. Then it was passed through a glass water trap to remove condensed water, and, finally, through two columns, one packed with glass wool, to remove small spray droplets, and another packed with anhydrous calcium chloride. Part of this air stream was then passed through saturating vessels; these were, however, not held in constant temperature baths. The humidity of the air stream was adjusted as in the 35<sup>°</sup>C. work. During the course of any particular experiment, the temperature of the air stream was measured periodically. Although the room temperature was maintained at 2 plus or minus 0.2<sup>°</sup>C., it was found that the temperature of the air stream could not be lowered to this temperature, but remained quite constant at 9 plus or minus 0.3<sup>°</sup>C. Using freshly packed drying towers, it was possible to attain relative humidities below 5% - the limit of the sensing elements - nominally

listed in the results as "0" relative humidity, because the recorder indicated a reading of 0. The maximum humidity attained was 96%.

Entirely new apparatus was designed and constructed for the work at 60 °C: because such an elevated temperature could not be achieved within the constant temperature room, it was decided that those portions of the apparatus enclosing the air stream and the fibre should be surrounded by thermostating jackets. The chambers enclosing the fibres were constructed from brass. Provision was made for clamping the fibres at 10.13 and 40.25 cms. from either end of the solenoid spindle. At these positions, windows were inserted so that the clamps, operable from without, could be screwed tightly together without causing any lateral displacement of the fibre. In order to have approximately the same number of determinations of the mechanical properties per experiment a number of additional weights to alter the mass of the vibrator assembly were constructed.

As some of the lower humidity range Aminco-Dunmore Electric Hydrometer elements in the wide range humidity sensing apparatus<sup>47</sup> could not be exposed to air whose dew point exceeds 110 °F., the Aminco-Dunmore narrow range high sensitivity humidity sensing elements<sup>48</sup> . Each high sensitivity element responds to humidities within a particular humidity range, so that, with some overlap between the elements, one can measure any humidity desired. As no calibrations for 140 °C. were provided, the elements were calibrated by extrapolating data provided within the temperature range 40 - 120 °F.,<sup>49</sup> as advised by the Aminco-Dunmore engineering department.

As in previous experiments, the humidity of the air stream was adjusted by combining a dried and a wet stream of air in appropriate proportions. The wet air was obtained by passing compressed air through the saturating vessels as before, but this time the oil bath temperature was maintained at 75 °C. The two air streams were combined in an air manifold immersed in the water circulating bath maintained at 60.0 plus or minus 0.05 °C. After passing through a heat exchanger also immersed in the water bath, the air was sent by means of water-jacketed rubber conduits to the humidity measuring chamber, whence it was led, again by means of water-jacketed rubber conduit, into the chambers surrounding the filaments. Water was circulated throughout the system by means of an Eastern Industries pump of 8 gallons per minute capacity. The temperature drop throughout the system was less than one degree.

It was found that at higher humidities -- above 55 % -- water from the air stream leaving the chambers surrounding the filaments condensed on the mcuh cooler transducer assembly, altering its mass. In order to overcome this difficulty, a stream of compressed air was made to flow at each end of the transducer assembly, in such a way as to deflect the moist air emanating from the chambers, thereby preventing condensation of water on the transducer. As this air flow interfered in the determination of the mechanical properties, it was shut off whenever a reading was taken. Any small amount of water that condensed on the transducer during the course of a determination was wiped off with cotton wool.

Two filaments, of the same material, each about 75 cm long, were attached one to each end of the vibrator spindle, making a symmetrical arrangement of two test pieces lying horizontally one on each side

of the transducer and coaxial with it. Each filament was tensioned at its end remote from the vibrating spindle by gram weights approximately equal to half the denier value of the filaments, e. g., 8 g for 15 denier nylon, and allowed to creep under this applied load for sixteen to twenty hours before the experiment, and was kept under this tension during the experiment. During the tensioning and conditioning period -- usually over night -- control of the humidity was usually within 5 % of the required humidity. Just preceding, and during the actual vibrational experiment, the humidity was manually adjusted, if necessary, to the required humidity. Overall variation in the humidity during the actual experiment was 1 to 2 %, depending on the temperature.

In all experiments, the vibrational amplitude was approximately 0.15 % strain. In most cases, several determinations of the mechanical properties, on different filaments, were made. When sufficient data, usually three runs, had been gathered at a given humidity, the humidity was increased by about 10 %. The entire humidity range was scanned in this way. The results were plotted in rough fashion in order to keep track of the changes in the properties with humidity, and, if conditions warranted, experiments were performed at intermediate humidities.

During the actual experiment, the resonant frequency of the system, the vibrational amplitude, and the current required for that amplitude were recorded. At 35 °C, the temperature and humidity were recorded as well; at 9 °C, relative humidity only. At these two temperatures, the humidity during the course of the experiment was determined as the average of these readings. At 60 °C, the average relative humidity was obtained by integrating the area under the recorder trace.



The resonant frequency of the system was altered by changing the length of the filament clamped, and by increasing the mass on the vibrating spindle. The latter method merely required placing small weights from 2 to 100 g on the vibrating spindle. Using these methods, it was possible to obtain readings over somewhat more than one cycle of logarithmic frequency.

#### B. Calibration of the Solenoids and Determination of Parameters.

The solenoids, or vibrator units, were calibrated so that the force they exerted could be determined from the current flowing through them. To do this, the magnet-vibrator assembly was set up vertically in such a way that the vibrator unit could be suspended freely in the magnetic gap by a linear calibrated spring. The vibrator was centered within the magnetic gap, and was then loaded with a succession of analytical weights. The vibrator was brought back to its unloaded position by passing direct current through the solenoid coil. The force could be calculated from the equation  $F = Mg + K\Delta x$ , where  $M$  is the added mass,  $g$ , the gravitational constant;  $K$ , the modulus of the spring, and  $\Delta x$  is the distance between loaded and unloaded positions of the vibrator unit. Experimentation showed, however, that the corrections resulting from differences in the exact positions of the vibrator unit between the loaded and unloaded positions could be neglected, as these corrections amounted to only a few tenths of one percent, at the very most. Accordingly,  $F = Mg$  was considered to give a value sufficiently close to the actual value. A plot of  $F$  against  $i$ , the current in milliamperes, will give a straight line of slope  $\mathcal{F}$  dynes per milliampere. An alternating current whose root mean square value, read off the alternating current milliampere, is  $i$  exerts a maximum force  $F_{\max} = \sqrt{2}\mathcal{F}i$ . It is this maximum force which is used in the calculation of  $E^0$ .

Two different vibrator assemblies were constructed during the course of this work. The first assembly's main coil was accidentally burned out midway in the 9 °C work. Both consisted of three solenoid coils: one large, of about 90 to 95 turns, a smaller coil of 25 to 30 turns, and another, smaller yet, of 1 to 2 turns. In the calibration of the large coils, 1 to 8 g weights were used; for the medium coils, 0.1 to 1.0 g weights; and for the small coils, 10 to 100 mg weights. Data concerning the number of turns and the calibration factor in dynes per milliampere are reported in Table I.

Table I. Coil Calibrations.

First Assembly		Second Assembly	
Number of turns	Calibration Factor	Number of turns	Calibration Factor
	dyne/ma.		dyne/ma.
93	50.0	90	60.2
25	12.09	30	20.3
2	1.29	2	1.40

When the solenoid had been calibrated, the effective mass  $M$  of the transducer could be calculated from the equation of motion:

$$M \frac{d^2x}{dt^2} + R \frac{dx}{dt} + Px = F_{\max} \cos \omega t \quad (2)$$

$$\text{where } R = \frac{2A}{l} \eta + R_1 \quad (3)$$

$$\text{and } P = \frac{2A}{l} E' + P_1 \quad (4)$$

$P_1$  is a correction factor for the vertical displacement of the vibrator unit during horizontal vibration, and is given by  $P_1 = Mg/h$ , where  $M$  is the mass of the system,  $g$  is the gravitational acceleration, and  $h$  is the suspension height.  $R_1$  is a correction factor for dissipative forces other than those present in the filaments. It is given by  $R_1 = F/\omega_x$ , at resonance,

where  $F$  is the force required to produce  $x$ , the vibrational amplitude, at the resonant frequency  $\omega_r$ .

The steady state solution of the equation is

$$x = \alpha' \cos \omega t + \beta' \sin \omega t \quad (5)$$

$$\text{where } \alpha' = \frac{F_{\max} (M\omega^2 - P)}{(M\omega^2 - P)^2 + R^2\omega^2} \quad (6)$$

$$\text{and } \beta' = F_{\max} R\omega / \{(M\omega^2 - P)^2 + R^2\omega^2\} \quad (7)$$

Differentiation with respect to time, and use of equations (6) and (7) shows that

$$x_{\max} = F_0 / \{(M\omega^2 - P)^2 + R^2\omega^2\} \quad (8)$$

$R^2\omega^2$  is negligible compared to  $(M\omega^2 - P)$  for values of  $\omega$  which are not too close to  $\omega_r$ . Hence a plot of  $\pm F/x$  against  $\omega^2$  should give a curve which deviates from a straight line only near resonance, the slope of the line being  $M$ , the effective mass of the vibrating system. Results of effective mass determinations are reported in Table II.

Table II. Mass Calibrations.

First Assembly		Second Assembly	
Effective Mass	Weighed Mass	Effective Mass	Weighed Mass
M, in grams.	gram	M, in g.	g
4.09	4.08	4.51	4.40
24.64	25.04	16.6	16.1

Several mass calibrations were performed on each of the two vibrator assemblies. Difficulties were encountered in obtaining results that agreed reasonably well with the known, or "weighed" weights of the vibrator

assemblies. A glance at Table II reveals that the effective mass is not necessarily identical to the weighed mass of the system. Effective mass is the mass determined by the method just elaborated, and weighed mass is the mass of the vibrator assembly obtained by adding all the weights of the components of the assembly.

The correction factor  $P_1$  was evaluated simply by measuring  $M$  and  $h$ , and using  $g$  equal to 981 dynes /sec.<sup>2</sup> The  $R_1$  factors were determined by a forced vibration method. Values obtained are reported in Tables III and IV. The values reported for  $R_1$  in the first column in Table III were obtained by plotting  $x/F$  versus  $\omega$  and drawing smooth curves through the points. This method was not deemed satisfactory, as the uncertainty in the exact position of the inflection point was very great; sometimes this uncertainty amounted to 20 %. Accordingly, subsequent values

Table III.  $R_1$  Correction Factors for First Transducer Assembly.

Total weight of transducer assembly and added mass.	$R_1$ factor, in dyne-sec./cm, evaluated for experiments at	
	35 °C	60 °C
gram		
4.09	3.10	1.98
9.81	2.38	2.04
15.53	2.44	1.90
29.38	2.15	2.29
40.83	2.63	1.97
54.50	2.77	2.00 (est.)
79.79	3.64	--

reported in Tables III and IV were determined by tuning directly to resonance, and measuring  $F$  and  $x$  directly at resonance. This method was found to be entirely satisfactory. The high values reported in the first column of Table IV were obtained for the assembly with coiled leads going

from the solenoid coils to fixed terminals placed on top of the magnet.

The lower values reported in the second column were obtained for straight leads simply curved upwards from the solenoid terminals to the fixed terminals on the magnet.

Table IV.  $R_1$  Correction Factors for Second Transducer Assembly.

Total weight of transducer assembly and added mass.	$R_1$ factor, in dyne-sec./cm, evaluated for experiments at	
	9 °C.	60 °C.
gram		
4.51	5.35	1.82
6.77	--	2.00
8.40	--	2.02
10.23	3.84	1.73
13.63	--	1.91
14.12	3.58	1.91
15.96	--	1.68
19.35	--	1.65
25.1	--	1.88
29.8	3.55	1.59
41.2	4.82	1.96
55.1	4.44	2.72
80.2	--	2.37
105.3	--	3.49

## RESULTS

The dynamic modulus  $E'$  of nylon is plotted as a function of logarithmic frequency at a number of relative humidities at 9, 35 and 60 °C. in Figures 3, 4 and 5 respectively. Inspection of the 9 °C. results shows that, in most cases, the dynamic modulus increases with increasing frequency. This increase is not so great as that reported by Fujino et al.<sup>21</sup> for Nylon 6. It is not at all clear why the modulus decreases with increasing frequency in the region 19 to 60 % r.h. A closer examination of the results at any humidity within the range shows that some experiments exhibit an increase in  $E'$  with increasing frequency. The forementioned affect may be spurious, for the slopes observed at higher humidities might lead one to believe that only a decrease in slope to zero, followed by an increase, to rather large values, with increasing relative humidity may occur. The results are not sufficiently precise, however, to permit detailed analysis. The 35 and 60 °C. results for the dynamic modulus show more regularity: the modulus increases with increasing frequency at all humidities. The change in slope with increasing humidity does not appear to follow a regular pattern, as may be seen by inspection of Table V.

It was found that, although individual runs were fairly consistent within themselves, showing only small deviations from linearity, difficulty was experienced in reproducing these values, at the same humidity. Examination of the results at 35 °C. and 63 % r.h. shows that the two runs do not superimpose at all. Results for each run were plotted against logarithmic frequency; and the best straight line drawn through them. These straight lines were averaged to give the lines reported on the graphs.

Table V. Slopes of  $E'$  against log graphs, in dynes/cm<sup>2</sup> x 10<sup>-10</sup>.

9 °C.		35 °C.		60 °C.	
r.h.	Slope	r.h.	Slope	r.h.	Slope
0	0	11.0	- 0.30	10.5	- 0.39
5.4	- 0.11	12.8	- 0.21	18.3	- 0.62
9.5	- 0.05	22.5	- 0.30	20.5	- 0.63
16.3	- 0.04	31.1	- 0.24	25.1	- 0.55
19.0	- 0.09	39.4	- 0.31	28.2	- 0.47
30.0	- 0.18	44.1	- 0.23	35.4	- 0.44
38.3	- 0.05	50.7	- 0.38	37.9	- 0.44
48.2	- 0.02	51.8	- 0.23	41.0	- 0.48
51.0	0	56.2	- 0.54	51.2	- 0.54
58.4	- 0.05	63.0	- 0.42	57.2	- 0.32
67.6	- 0.44	67.7	- 0.35	59.8	- 0.19
76.0	- 0.28	69.7	- 0.46	63.4	- 0.18
86.0	- 0.66	80.5	- 0.26	70.7	- 0.32
88.3	- 0.66	82.7	- 0.46	76.0	- 0.18
93.5	- 0.50	89.2	- 0.17	85.0	- 0.16
		96.0	- 0.18	93.8	- 0.34

These straight lines may, in some cases, not appear to be the best straight lines that could be drawn: it must be remembered nevertheless that a number of experimental points could not be reported in the graphs, as they overlapped one another. This situation is especially true with respect to those determinations in which three or more runs were made.

The energy loss  $E''$  is plotted as a function of log-

arithmetic frequency at a number of relative humidities at 9, 35, and 60 °C. on Figures 6, 7, and 8 respectively. It would appear that at 9 °C.  $E''$  increases with frequency at low humidities. Within the range 40 to 60 % r.h., the energy loss appears to be constant with frequency, and then, at higher humidities, decreases with increasing frequency. At 35 °C., the energy loss decreases with increasing frequency at low humidities, appears to be constant with increasing frequency within the range 50 - 70 % r.h., and increases with increasing frequencies at higher humidities. The same type of behaviour is shown by the 60 °C. experiments. At humidities below 40 %, the energy loss decreases with increasing frequency; in the range 40 to 65 % r.h., it appears to be insensitive to frequency, whereas at humidities in excess of 65 %, it appears to increase again with increasing frequency. These conclusions may be checked by examining the values for the slope of the graphs of  $E''$  against  $\log \omega$  in Table VI.

The slopes of the energy loss versus logarithmic frequency curves do not appear to increase with increase in relative humidity. This behaviour may be due to the scatter within the experiments. The lines drawn throughout the data for  $E''$  were obtained by plotting the data as  $\log \eta$  versus  $\log \omega$ , plotting all results at one temperature and humidity on one graph, and drawing the best straight line through the points. These plots give rather better straight lines (See Figures 9 to 17.) than would appear from Figures 6 to 8. Values of  $\eta \omega$  ( $E''$ ) were evaluated at arbitrarily chosen values of  $\omega$ , and were plotted on the  $E''$  versus  $\log \omega$  graphs, to give the straight line reported in the results. The full lines drawn into Figures 9 to 17 represent the best straight lines that can be drawn through the points; the dotted lines represent  $E'' = \text{constant}$  lines, included for purposes of comparison.



Table VI. Slopes of  $E''$  against log graphs, in dynes/cm<sup>2</sup> x 10<sup>-9</sup>.

9 °C.		35 °C.		60 °C.	
r.h.	Slope	r.h.	Slope	r.h.	Slope
0	- 0.35	11.0	- 0.23	10.5	- 0.54
5.4	- 0.31	12.8	- 0.22	18.3	- 0.53
9.5	- 0.30	22.5	- 0.18	20.5	- 0.36
16.3	- 0.17	31.1	- 0.30	25.1	- 0.32
19.0	- 0.22	39.4	- 0.24	28.2	- 0.36
30.0	- 0.11	44.1	- 0.21	35.4	- 0.16
38.3	- 0.24	50.7	- 0.02	37.9	- 0.22
48.2	- 0.09	51.8	- 0.02	41.0	- 0.05
51.0	0	56.2	0	51.2	- 0.29
58.4	- 0.08	63.0	- 0.02	57.2	- 0.14
67.6	- 0.12	67.7	- 0.24	59.8	- 0.48
76.0	- 0.04	69.7	- 0.14	63.4	- 0.05
86.0	0	80.5	- 0.27	70.7	- 0.44
88.3		82.7	- 0.32	76.0	- 0.29
93.5	- 0.65	89.2	- 0.21	85.0	- 0.13
		96.0	- 0.30	93.8	- 0.19

Figures 18 and 19 report the dynamic modulus as a function of relative humidity at two arbitrarily chosen frequencies,  $\omega = 20$ , and  $\omega = 150$ , respectively. The former represents the lower frequency extremity; the latter, the upper frequency extremity. Comparison of these two figures shows that, for 35 and 60 °C., the modulus increases with increasing frequency for all relative humidities, whereas at 9 °C., the modulus is insensitive to frequency changes up to about 50 % r.h., but

then starts to decrease, rather sharply, with increasing humidity.

Figures 20 and 21 report energy loss as a function of relative humidity at  $\omega = 20$  and  $\omega = 150$ . The average value of  $E''$  increases with increasing humidity at all humidity values, at 9 °C. At 35 and 60 °C., the behaviour is more complex; it leads to a shift in the position of the maximum peaks. At 35 °C., the peak shifts from 55 % r.h. at  $\omega = 20$  to 64 % r.h. at  $\omega = 150$ . Similarly, at 60 °C., the peak shifts from 33 % r.h. at  $\omega = 20$  to 44 % r.h. at  $\omega = 150$ .

The values of  $E'$  and  $E''$  evaluated at  $\omega = 150$  are plotted versus the amount of water adsorbed at equilibrium by nylon at the humidities studied, on Figures 23 and 24. Values for water adsorption were obtained by extrapolation of Bull's data, assuming linear relations. The data so obtained are plotted on Figure 22. Strictly speaking, extrapolation of Bull's data is not justifiable. The error introduced, however, is probably not very great.<sup>50</sup>

## DISCUSSION

Schmieder and Wolf<sup>32</sup> have examined the mechanical properties of various nylons, over a wide temperature range and at very low frequencies, and report energy loss maxima in three regions, with indications of an increase in energy loss above 200 °C., with the onset of melting. For nylon 66, the three maxima occur at about 153, 223, and 338 °K. These dispersion regions are usually referred to as the  $\tau$ ,  $\beta$ , and  $\alpha'$  dispersion regions respectively, and the region about the melting point is referred to as the  $\alpha$  dispersion region. The  $\alpha$  region in the energy loss curves arises from the enhancement of chain mobility resulting from melting of crystallites. The other peaks are believed to arise from cooperative motions of either stressed or unstressed segments of the polymer chains in the amorphous regions. Table VII lists the activation energies Schmieder and Wolf calculate for motion in the various dispersion regions, for both nylon 6-6 and nylon 6-10, evaluated by low frequency methods. ( $\sim 1$  c.p.s.)

Table VII. Activation Energies calculated for nylon 6-6 and nylon 6-10 by Schmieder and Wolf.

Dispersion Region	Temperature °K.	Energy of Activation of Viscous Flow kcal./mole.	
		Nylon 6-6	Nylon 6-10
$\alpha'$	350	73	163
$\beta'$	250	21	19-27
$\tau$	170	21	20

These values suggest that the  $\alpha'$  dispersion is quite different from either the  $\beta$  or the  $\tau$  dispersion, which Schmieder and Wolf believe arise from mechanisms not too different from one another. The suggestion of Sauer et al.<sup>29,30</sup> that the  $\alpha'$  dispersion may result from the onset of motion of large chain segments in the amorphous regions seems therefore reasonable.

It is believed that the  $\gamma$  peak results from the onset of cooperative movement of  $\text{CH}_2$  groups within the polymer chain. This peak has also been observed in polyethylene and in certain methacrylates. The origin of the  $\beta$  peak is not at all clear. However, Sauer and co-workers suggest that the  $\beta$  region in the polyamides is due to segmental motion in the amorphous region involving amide groups not hydrogen bonded to other amide groups. on the other hand, in polyethylene, this peak is believed to arise from motion of side groups<sup>28,45</sup> Similar dispersion phenomena have been observed for teflon, polyethylenes, and some methacrylates. All four dispersion regions are not necessarily observed in every substance, however. The  $\alpha'$  peak is usually referred to as the primary absorption maximum; the  $\beta$  and the  $\gamma$  peaks, as secondary absorption maxima.

Woodward, Sauer, Kline and Deeley<sup>29,30</sup> have examined the damping factor (  $\tan \delta \ E''/E'$  ) versus temperature maxima for nylon 6-6 and have reported a marked dependence of both the magnitude of the maximum and the temperature at which the maximum occurs on the water content. In their experiments, they used rods of nylon approximately 0.6 to 0.8 cm in diameter and 10 to 11 cm long. Examination of Figure 2 of their results gives the following data for 308 and 333 °K.:

Table VIII. Comparison between the Results obtained in this investigation and Results reported by Sauer and coworkers.

Treatment	Estimated Humidity	$\tan \delta$			
		308 °K.		333 °K.	
		Sauer	Present Results	Sauer	Present Results
16 mos in desiccator	0 %	0.012	0.016	0.054	0.012
As received	40 %	0.036	0.031	0.111	0.045
3 weeks at 100% r.h.	100 %	0.070	0.036	0.01	0.018

One should not very great significance to these

results, however, since the penetration of water to the inner portions of the nylon rods has not been established. The values listed in the column "estimated Humidity" are not Sauer's. The values quoted in the Table as "Present Results" were evaluated at  $\omega = 150$ , and at the stated temperature and humidity. Comparison between these values and those of Sauer show that there exists a general agreement between their and the present work -- the trends are the same. One should not expect detailed agreement, as the frequencies at which Sauer evaluated these results were in the range 600-1,000 c.p.s. The maximum values of  $\tan \delta$  reported in this work are greater than the values of  $\tan \delta$  for the  $\beta$  peak reported by Sauer<sup>29</sup>, and even approach the values reported by him for the  $\alpha'$  dispersion. It seems therefore that we are dealing with the  $\alpha'$  dispersion, even at lower temperatures.

In order to have a reasonable basis for comparison, it is desirable to convert relative humidities at any temperature to the amount of water sorbed by a given weight of polymer. Accordingly, in the ensuing discussion, the graphs of  $E'$  and  $E''$  against moisture content (Figures 23 and 24) will be used.

The results obtained for the energy dissipation versus moisture content can easily be explained qualitatively. Let us consider the results at 60 °C. At very low water contents, the energy loss is low because chain mobility is restricted by the existence of many hydrogen bonds. As the weight of water sorbed increases, more hydrogen bonds are broken, segmental motion is facilitated, and the energy dissipation increases, because more chains can flow. Simultaneously, the force required to move a chain segment will decrease with decreasing chain inter-

action, and a maximum will be set on the energy dissipation by this particular mechanism. As still more water is sorbed, chain interaction is further decreased, and the energy loss will then decrease. One would therefore expect a maximum in  $E''$  to occur at some intermediate degree of freedom of motion of the chains in the amorphous region in the same way that loss maxima occur at an intermediate point in the rubber-to-glass transition range. The proposed mechanism is accompanied by the decrease in modulus that one would expect when chain interactions become weaker.

The 35 °C. energy loss data may be explained in much the same way as the 60 °C. data. The 9 °C. data can not be explained on this basis, without some modification -- one can fit the data only to the first half of the proposed mechanism. Thus, the results at  $\omega = 150$  would seem to indicate that  $E''$  increases continuously with increasing moisture content, and that  $E'$  decreases beyond 40 % r.h. These results would suggest that, as increasing amounts of water are sorbed, molecular motion is freed, but that this freeing of molecular segments is still incomplete at the highest value of water sorption, so that no maximum is observed. This maximum could therefore be thought of as lying beyond the 100 % r.h. range. The results at  $\omega = 20$  (Figure 20) seem to indicate that an energy loss maximum does exist in the vicinity of 90 % r.h. If the energy loss does indeed exhibit a maximum, albeit at lower frequencies, the results could be explained in a manner analogous to the explanation proposed for the results at the higher temperatures.

There remains the question of why the energy loss maximum should move to lower humidities as the temperature is raised. This question can probably be explained quite satisfactorily by taking into account the difference in temperature between the different determinations. Thus, as the temperature increases, the thermal energy of the chain seg-

ments will increase, so that the same amount of chain motion can be achieved with less breaking of hydrogen bonds, that is to say, more hydrogen bonds are weakened or broken by thermal agitation at higher temperatures than at lower temperatures, and therefore fewer hydrogen bonds have to be broken by sorbed water, with the result that, as the temperature is raised, the energy loss peak moves to lower moisture content values.

Various workers have suggested that an increase in relative humidity corresponds qualitatively to an increase in frequency for the process, and vice versa. Accordingly, when the energy dissipation is evaluated at  $\omega = 20$  rather than at  $\omega = 150$ , one should expect the maxima in energy dissipation to shift in the direction of lower humidities. Inspection of Figures 20 and 21 will show that this principle appears to hold for nylon 6-6. A shift in  $\omega$  from 150 to 20 causes the energy loss maximum to shift from 63 to 55 % r.h. at 35 °C., and from 42 to 33 % r.h. at 60 °C.

An attempt to evaluate the activation energy for the viscous flow process was made with the method of Ferry<sup>6</sup> in which he calculates values for the apparent activation energy for viscous flow for a number of polymers using the relations

$$\left( \frac{\partial \ln E'}{\partial T} \right)_{\omega} = \left( \frac{\partial \ln E'}{\partial \ln a_T} \right)_T \left( \frac{\partial \ln \omega a_T}{\partial T} \right)_{\omega} \quad (9)$$

$$\text{and} \quad \Delta H_a = R \frac{\partial \ln a_T}{\partial \left( \frac{1}{T} \right)} \quad (10)$$

where  $E'$  is the real part of the dynamic modulus,  $a_T$  is the temperature reduction factor used to reduce values of  $E'$  and  $E''$  to one arbitrarily chosen temperature, using the time-temperature superposition principle,

R is the gas constant in kcal./mole-°C., and  $\Delta H_a$  is the activation energy for viscous flow. In order to apply these relations to the present results, equations (9) and (10) were modified to: (See Appendix.)

$$\Delta H_a = \frac{AR}{\phi (-\ln w)} \frac{dE'}{d(\frac{1}{T})} \quad (11)$$

where A is a gamma function defined in terms of experimentally determinable quantities. If one knows the value of A,  $\phi$  and  $dE'/d(\frac{1}{T})$  one can calculate  $\Delta H_a$ . Plots of  $E'$  against  $1/T$  at various constant water content values seemed to indicate essentially two slopes, for the data were not sufficiently precise to allow further discrimination between the slopes. The slopes of the lines for which the water content was less than 2.4 g. water per 100 g. nylon all lay between  $3.70$  and  $4.06 \times 10^{13}$  dynes-°C./cm<sup>2</sup>, and were averaged to  $3.89 \times 10^{13}$  dynes-°C./cm<sup>2</sup>. At about 2.5 g water per 100 g of nylon, an intermediate slope of  $4.94 \times 10^{13}$  was recorded, and at water contents in excess of 4 g., two slopes,  $6.98$  and  $7.78 \times 10^{13}$  were obtained, and averaged to  $7.38 \times 10^{13}$  dynes-°C./cm<sup>2</sup>. The slopes were averaged in this way because it was felt that the methods used were not sufficiently precise to enable one to discriminate between the values. The function A was calculated for each humidity for which it was required, as described in the appendix. Table IX summarises the results for the apparent activation energy  $\Delta H_a$ . Activation energies listed by Ferry<sup>6</sup> for eight amorphous polymers such as rubbers, polyvinyl acetate and polymethylmethacrylate range from 14 to 82 kcal./mole. This would suggest that the values herein obtained, with the exception of the two values in excess of 100 kcal./mole, are not too unreasonable.

If increasing water content exerts a plasticising



effect upon the nylon, causing a breaking of hydrogen bonds in the amorphous regions, the general trend of the 9 °C. activation energies seems reasonable, although the magnitudes of some of the activation energies are somewhat alarming. It should be remembered also that at 282 °K., and high humidities, according to Sauer's results, the energy dissipation phenomenon would correspond to the  $\beta$  peak, with a  $\tan \delta$  maximum at 250°K. for the dessiccated sample. The increase in activation energy with increasing water sorption at 60 °C. might be explained on the basis of hydrogen bond rupture freeing far greater molecular segments. At this temperature one is working in the region of the  $\alpha'$  peak, for which reported activation energies are much greater. The 35 °C. results could then be explained on the basis of a transition from the behaviour at 9 °C. to the behaviour at 60 °C.

Table IX. Activation Energies for Viscous Flow, in kcal./mole.

Water Content g. water per 100 g nylon.	Activation Energies		
	9 °C.	35 °C	60 °C.
1.0	110	43.8	26.3
2.0	49.0	32.4	28.8
4.0	43.8	51.4	102

It is not clear at present what interpretation can be given to these results. It has been suggested that the first two grams of water adsorbed by Nylon 6 exists in the polymer as bound water.<sup>35</sup> It has not been established that such is the case for nylon 6-6, but if it were, then any water adsorbed below this limit could provide very little plasticisation, and one would expect little change in the value of the modulus.

Such would appear to be the case at 9 and 35 °C., but not at 60 °C., where the change in modulus at water contents lower than 2 g. per 100 g. nylon is very marked. It is believed that water is adsorbed only within amorphous regions.<sup>51</sup> Starkweather maintains that water tends to catalyse crystallisation in nylon.<sup>52</sup> If crystallinity were, in fact, greatly enhanced, one would expect an increase in modulus. Although the results do not show an increase in modulus with increasing water content, it is possible that this increase in modulus due to an increase in crystallinity is masked by the more pronounced enhancement of motion, due to breaking of hydrogen bonds by sorbed water in the amorphous regions.

Ferry<sup>53</sup> and Andrews<sup>54</sup> have both noted that if a polymer system is represented by an infinite array of relaxation mechanisms for which one can write some distribution function  $\phi(\tau)$ , then there exists a relation between the imaginary part  $E''$  of the complex modulus and the rate of change of the real part  $E'$  with frequency. This relation may be represented approximately by

$$E'' \approx dE'/d\log \omega \quad (12)$$

Inspection of Table V shows that, for most modulus determinations, the value is positive, and varies from values too small to be evaluated, to a large value of  $6.6 \times 10^9$  dynes/cm<sup>2</sup>. A closer examination of  $dE''/d\log \omega$  at 35 and 60 °C. also shows that there is general agreement in behaviour between  $E''$  and  $dE'/d\log \omega$ ; i.e., the latter also exhibits a maximum value at some intermediate humidity range. If one ignores the negative slopes at 9 °C. -- all except that for 30 % r.h. are sufficiently small to be questionable -- one might expect the energy loss to be constant in the low humidity region, and then to increase rather sharply. The results at this temperature are not sufficiently precise to permit more detailed treatment.

# APPENDIX

Equation (9) can be readily derived, not, as might be expected, from a function of the type  $E = f(\omega, T, a_T)$  but from a function of the type

$$\ln E' = f(\omega, \ln \omega a_T, T) \quad (13)$$

We know experimentally that  $\omega a_T = f(\omega, T)$  so that  $E' = f(\omega, T)$

By suitable partial differentiation we obtain

$$\left( \frac{\partial \ln E'}{\partial T} \right)_{\omega} = \left( \frac{\partial \ln E'}{\partial \ln \omega a_T} \right)_T \left( \frac{\partial \ln \omega a_T}{\partial T} \right)_{\omega} + \left( \frac{\partial \ln E'}{\partial T} \right)_{\ln \omega a_T} \quad (14)$$

The dynamic modulus can be plotted as a single curve against reduced frequency  $a_T$ . This curve applies to all temperatures. Therefore  $E'$  has a unique value, irrespective of temperature if it is considered as a function of reduced frequency. The last term in equation (14) is precisely the rate of change of  $E'$  with respect to temperature at constant reduced frequency, and is equal to zero:  $\left( \frac{\partial \ln E'}{\partial T} \right)_{\ln \omega a_T} = 0$

We therefore obtain

$$\left( \frac{\partial \ln E'}{\partial T} \right)_{\omega} = \left( \frac{\partial \ln E'}{\partial \ln \omega a_T} \right)_T \left( \frac{\partial \ln \omega a_T}{\partial T} \right)_{\omega} \quad (9)$$

It is desirable to modify equation (10) in such a way that it can be used to calculate activation energies from the present results.

$$\Delta H_a = R \frac{\partial \ln a_T}{\partial (1/T)} \quad (10)$$

Remembering that  $d(1/T) = -1/T^2 dT$ , (10) becomes

$$\frac{\Delta H_a}{RT^2} = - \frac{\partial \ln a_T}{\partial T}$$

Since  $\frac{\partial}{\partial T} (\ln \omega a_T)_\omega = \frac{\partial}{\partial T} (\ln a_T)$

we may write  $\frac{\Delta H_a}{RT^2} = - \frac{\partial \ln \omega a_T}{\partial T}$  at constant  $\omega$ .

Substituting this relation into (9)

$$\left( \frac{\partial \ln E'}{\partial T} \right)_\omega = \left( \frac{\partial \ln E'}{\partial \ln \omega a_T} \right)_T \left( - \frac{\Delta H_a}{RT^2} \right)_\omega$$

One definition of the distribution function for relaxation times is

$$\phi(-\ln \omega) = A E' d \ln E' / d \ln \omega \quad (15)$$

where  $\phi$  is the distribution function, and  $A$  is a gamma type correction factor, and is represented by equation (18).

Rearrangement of (15) yields  $d \ln E' / d \ln \omega = \phi(-\ln \omega) / A E'$

Remembering that  $d(\ln \omega a_T)_T = d \ln \omega$  since  $a_T$  is constant if  $T$  is constant:

Equation (9) becomes:

$$\left( \frac{\partial \ln E'}{\partial T} \right)_\omega = \frac{\phi(-\ln \omega)}{A E'} \left( - \frac{\Delta H_a}{RT^2} \right)_\omega$$

Rearrangement yields, at constant  $\omega$ ,

$$\Delta H_a = \left\{ A E' R T^2 / \phi(-\ln \omega) \right\} \left( \frac{\partial \ln E'}{\partial T} \right)_\omega$$

Since  $d \ln E' = dE' / E'$  and  $d(1/T) = -(1/T^2) dT$ , we finally obtain,

$$\Delta H_a = \frac{A R}{\phi(-\ln \omega)} \frac{dE'}{d(1/T)} \quad \text{at constant } \omega \quad (11)$$

Thus, one can calculate the apparent activation energy if one knows the value of the distribution function and knows the slope of a plot of dynamic modulus, at a fixed frequency, against the reciprocal of the absolute temperature. It must be noted that the applicability of the time-temperature superposition principle is assumed in this derivation. There are a number of ways whereby  $\phi(-\ln \omega)$  may be evaluated, for

$$\phi(-\ln \omega) = A E' d \ln E' / d \ln \omega \quad (15)$$

$$\phi(-\ln \omega) = B E'' (1 - d \ln E'' / d \ln \omega) \quad (16)$$

$$\phi(-\ln \omega) = B \omega \eta' d \ln \eta' / d \ln \omega \quad (17)$$

A and B are second approximation factors defined by

$$A = (2-m) / 2\Gamma(2 - \frac{m}{2}) \Gamma(2 + \frac{m}{2}) \quad (18)$$

$$B = (1+m) / 2\Gamma(\frac{3}{2} - \frac{m}{2}) \Gamma(\frac{3}{2} + \frac{m}{2}) \quad (19)$$

where m is the negative slope of a plot of  $\log \phi$  from a preliminary first approximation calculation against the log of the relaxation time  $\tau$ , or  $\omega^{-1}$ . The second approximation is satisfactory only if  $A \approx B \approx 1$ . m is ordinarily positive because  $\phi$  is usually a decreasing function of  $\tau$ .

The zeroth order approximation for  $\phi$  is given by

$\phi = E^*$ . The first order approximation is obtained by setting  $A = B = 1$ .

If m lies between 0 and 1, A and B lie between 0.5 and 1.0.

Distribution functions were calculated at a number of relative humidities at all temperatures. Distribution functions were first calculated at a number of relative humidities at 35 and 60 °C. using all three relations (15 to 17). Examination of these results seemed to indicate that the distribution function defined by the relation (17) was most sensitive to changes in humidity. The relation (18) was rejected because small changes in  $d \ln E^* / d \ln \omega$  would not materially alter the factor  $1 - d \ln E^* / d \ln \omega$ ; i.e.,  $\phi$  as thus defined is relatively insensitive in changes in the slope of  $\ln E^*$  against  $\ln \omega$  plots, at least for low values of the slope. Accordingly, distribution functions were calculated for all experiments using the relation (17): these distribution functions are reported versus relative humidity and moisture sorption on Figures 25 and 26 respectively.

## BIBLIOGRAPHY

1. Alfrey, T., Mechanical Behaviour of High Polymers, Vol. VI of High Polymers, New York: Interscience Publishers, Inc., 1948 pp 54 ff.
2. Eyring, H., H. J. White, G. Halsey, R. Stein, and C. H. Reichardt, Mechanical Properties of Textiles, Parts I to XI, Textile Research J. 15 295, 451 (1945); 16 13, 53, 124, 201, 329, 335, 378, 382, 635 (1946).  
  
Glasstone, S., K. J. Laidler, and H. Eyring, The Theory of Rate Processes New York: McGraw-Hill Book Company, Inc., 1941.  
  
Burte, H., G. Halsey, and J. H. Dillon, Textile Research J. 18 449 (1948).
3. For a recent review, see Tobolsky, A. V., J. Appl. Phys. 27 673 (1956).
4. Kuhn, W., Helv. Chim. Acta. 30 307, 464, 839 (1947).
5. Becker, R., Probleme der technischen Magnetisierungskurve, Berlin: Springer Verlag, 1938.
6. Ferry, J. D., J. Am. Chem. Soc. 72 3746 (1950).  
  
For a recent review, see Ferry, J. D., Structure and Mechanical Properties of Plastics, in Die Physik der Hochpolymeren, Vol. IV. Berlin: Springer Verlag, 1956 pp. 372 ff.
7. Child, W. C., and J. D. Ferry, J. Colloid Science 12 389 (1957), and preceding papers.
8. Leaderman, H., Elastic and Creep Properties of Filamentous Materials and Other High Polymers. Washington, D. C.: Textile Foundation, 1943.
9. Harris, M., L. R. Mizell, and L. J. Fourn, J. Research Natl. Bur. Standards 29 73 (1942)
10. Speakman, J. B., J. Textile Inst. 38 T102 (1947)
11. Meredith, R., J. Textile Inst. 36 T107 (1945)
12. Tobolsky, A. V., and E. Catsiff, J. Polymer Sci. 19 111 (1956).  
  
Tobolsky, A. V., and J. R. McLoughlin, J. Phys. Chem. 59 989 (1955)  
  
Catsiff, E., J. Offenbach, and A. V. Tobolsky, J. Colloid Sci. 11 48 (1956)

13. Nolle, A. W., J. Appl. Phys. **19** 753 (1948); J. Polymer Sci. **5** 1 (1950).
14. Ashworth, J. N., and J. D. Ferry, J. Am. Chem. Soc. **71** 662 (1949).  
Smith, T. L., J. D. Ferry, and F. W. Schremp, J. Appl. Phys. **20** 144 (1949).
15. Witte, R. S., D. G. Ivey, B. A. Mrowca, and E. Guth, J. APPL. Phys. **20** 481, 486 (1949).
16. Dillon, J. H., I. B. Prettymann, and G. L. Hall, J. Appl. Phys. **15** 309 (1944).  
Dillon, J. H., and S. D. Gehman, India Rubber World **115** 61, 217 (1946).
17. Dunell, B. A., and J. H. Dillon, Textile Research J. **21** 393 (1951).  
Tobolsky, A. V., B. A. Dunell, and R. D. Andrews, Textile Research J. **21** 404 (1951).  
Dunell, B. A., and G. Halsey, Textile Research J. **18** 178 (1948).
18. Gehman, S. D., D. E. Woodford, R. B. Stambaugh, and P. J. Jones, Ind. Eng. Chem. **33** 1032 (1941); **35** 694 (1943).
19. Lyons, W. J., Textile Research J. **19** 123 (1949).
20. Ballou, J. W., and J. C. Smith, J. Appl. Phys. **20** 493 (1949).
21. Fujino, K., H. Kawai, and T. Horino, Textile Research J. **25** 722 (1955).
22. Hamburger, W. J., Textile Research J. **18** 102, 705 (1948).
23. Hammerle, W. G., and D. B. Montgomery, Textile Research J. **23** 595 (1953).
24. Williams, M. L., and J. D. Ferry, J. Polymer Sci. **11** 169 (1953).
25. Meredith, R., Mechanical Properties of Textile Fibres New York: Interscience Publishers, Inc., 1956 pp. 77 ff.
26. Halsey, G., H. J. White, and H. Eyring, Textile Research J. **15** 295 (1945).
27. Sauer, J. A., and D. E. Kline, J. Polymer Sci. **18** 491 (1955).  
Woodward, A. E., C. W. Deeley, D. E. Kline, and J. A. Sauer, J. Polymer Sci. **26** 383 (1957); **28** 109 (1958).
28. Kline, D. E., J. A. Sauer, and A. E. Woodward, J. Polymer Sci. **22** 455 (1956).

29. Woodward, A. E., J. A. Sauer, C. W. Deeley, and D. E. Kline,  
J. Colloid Sci. 12 363 (1957).
30. Deeley, C. W., A. E. Woodward, and J. A. Sauer, J. appl. Phys. 28 1124  
(1957).
31. Fitzgerald, E. R., J. Chem. Phys. 27 1180 (1957).
32. Schmieder K., and K. Wolf, Kolloid Zeitschrift 134 149 (1953).  
Fuchs, O., H. Thurn, and K. Wolf, Kolloid Zeitschrift 156 27 (1958).  
Wolf, K., and K. Schmieder, Ricerca Scientifica 25A 732 (1955)  
Proceedings of the International Symposium on Macromolecular  
Chemistry, Turin, Italy, 1954. Distributed in North America  
by Interscience Publishers, Inc., New York.
33. Price, S. J. W., and B. A. Dunell, J. Polymer Sci. 18 305 (1955).
34. Bueche, F. M., J. Polymer Sci. 22 113 (1956).
35. Yoshitomi, T., K. Nagamatsu, and K. Kosiya, J. Polymer Sci. 27 335  
(1958).
36. Tokita, N., J. Polymer Sci., 20 515 (1956).
37. Price, S. J. W., A. D. McIntyre, J. P. Pattison, and B. A. Dunell,  
Textile Research J. 26 276 (1956).
38. Meyer, K. H., and W. Lotmar, Helv. Chim. Acta 19 68 (1936).  
see also Meredith, R., op. cit., p. 119.
39. Tokita, N., and K. Kanamaru, J. Polymer Sci. 27 255 (1958).
40. Fuoss, R. M., J. Am. Chem. Soc. 60 456 (1938); 61 2329, 2334 (1939);  
63 369, 378 (1941).  
Fuoss, R. M., and J. G. Kirkwood, J. Am. Chem. Soc. 63 385 (1941).
41. Davies, J. M., R. F. Miller, and W. F. Busse, J. Am. Chem. Soc. 63  
361 (1941).
42. Heyboer, J., Kolloid Zeitschrift 148 36 (1956).  
Jenckel, E., Kolloid Zeitschrift 136 142 (1954).
43. Hoff, E. A. W., Deutsch, K., and W. Reddish, J. Polymer Sci. 13 565  
(1954).
44. Hoff, E. A. W., D. W. Robinson, and A. H. Willbourn, J. Polymer Sci.  
18 161 (1955).



45. Oakes, W. G., and Robinson, D. W., J. Polymer Sci. 14 505 (1954).
46. Powell, R. W., Proc. Phys. Soc. 48 406 (1936).
47. American Instrument Company, Inc., Catalogue Number 4-4780.
48. American Instrument Company, Inc., Catalogue Number 4-4815 through 4-4822.
49. Quinn, F. C., private communication.
50. Bull, H. B., J. Am. Chem. Soc. 66 1499 (1944).  
see also Forward, M. V., and S. T. Smith, J. Textile Inst. 46 T158 (1955)  
as well as Abbott, N. J., and A. C. Goodings, J. Textile Inst. 40 7232 (1949).
51. Hailwood, A. J., and Horrobin, S., Trans. Faraday Soc. 42B 84 (1946)
52. Starkweather, H. W., Jr., G. E. Moore, J. E. Hansen, T. M. Roder, and R. E. Brooks, J. Polymer Sci. 21 189 (1956).
53. Ferry, J. D., E. R. Fitzgerald, M. F. Williams, and L. D. Grandine, J. Appl. Phys. 22 717 (1951).
54. Andrews, R. D., Ind. Eng. Chem. 44 707 (1952).



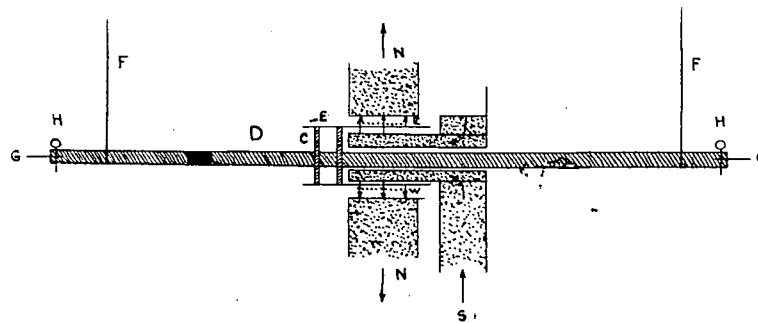
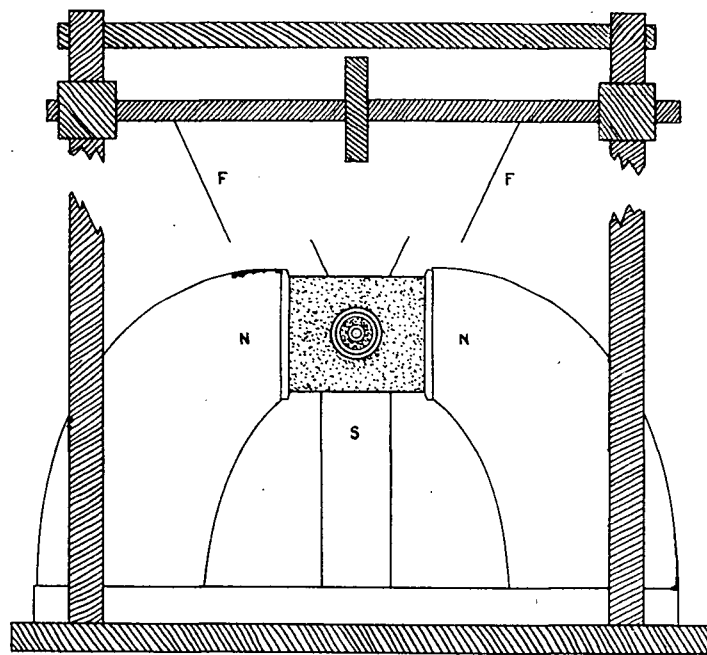


Figure 2. Detail of magnet assembly of filament vibrator and detail of vibrator unit showing the transducer coil.

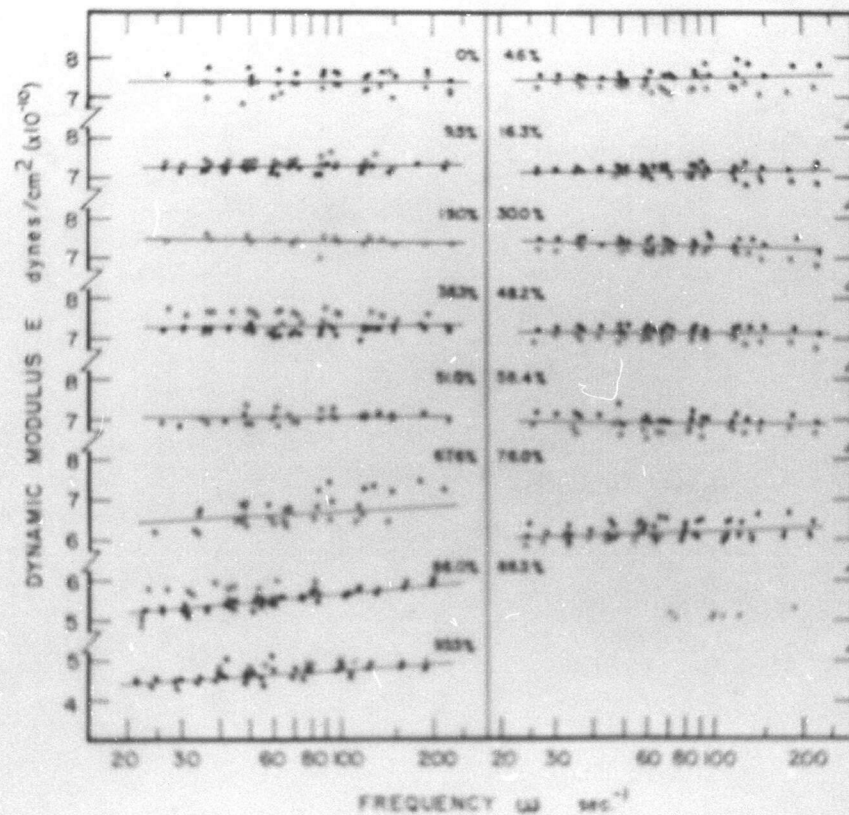


Figure 3. Dynamic modulus  $E'$  as a function of log frequency at 9 °C. and various humidities.

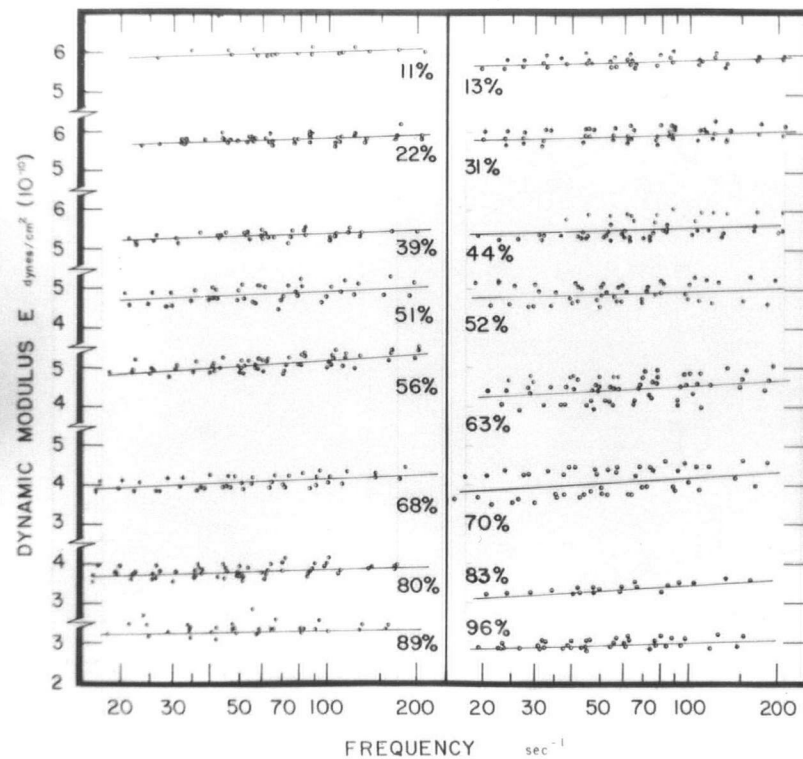


Figure 4. Dynamic modulus  $E'$  as a function of log frequency at 35 °C. and various humidities.

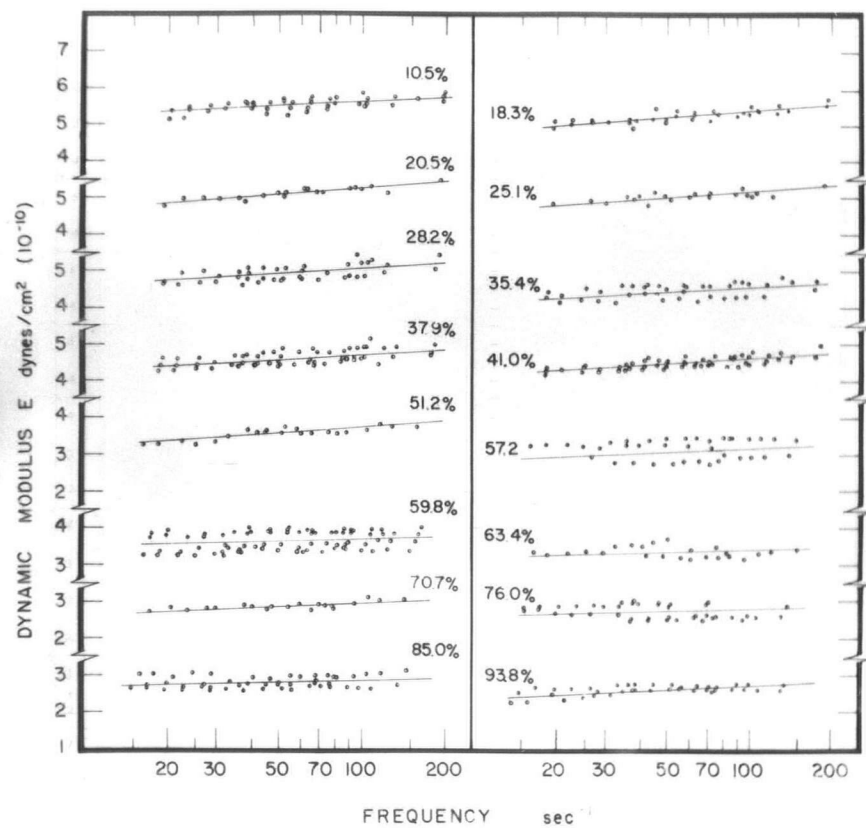


Figure 5. Dynamic modulus  $E'$  as a function of log frequency at 60 °C. and various humidities.

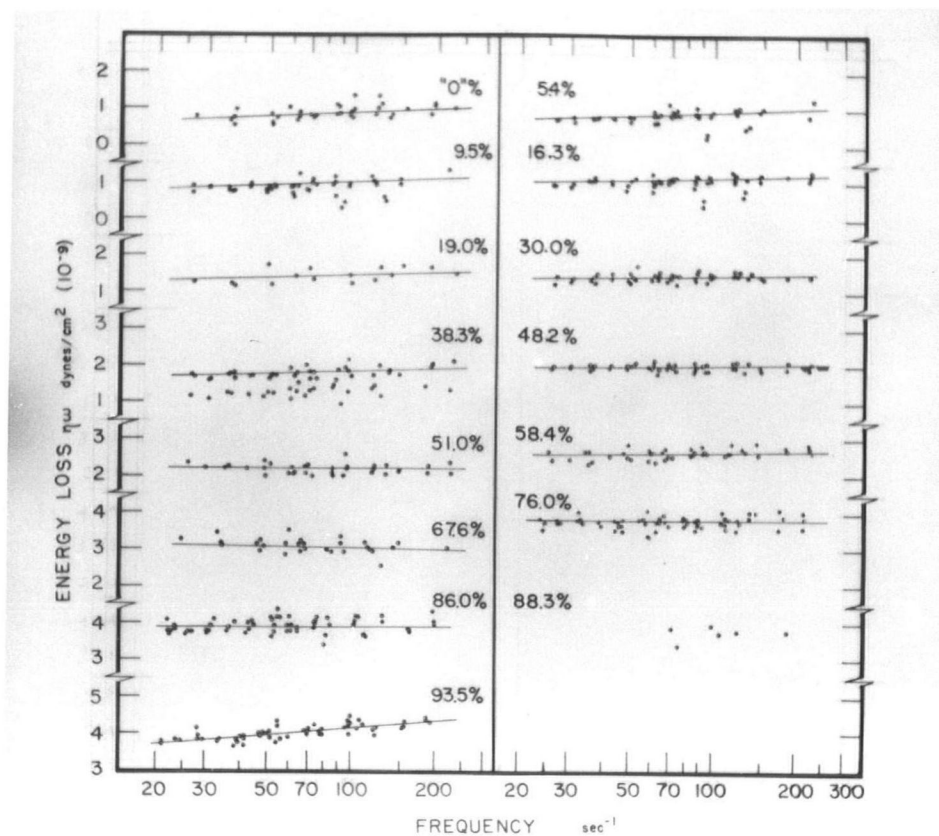


Figure 6. Energy Loss  $E''$  as a function of log frequency at  $9^\circ\text{C}$ . and various humidities.

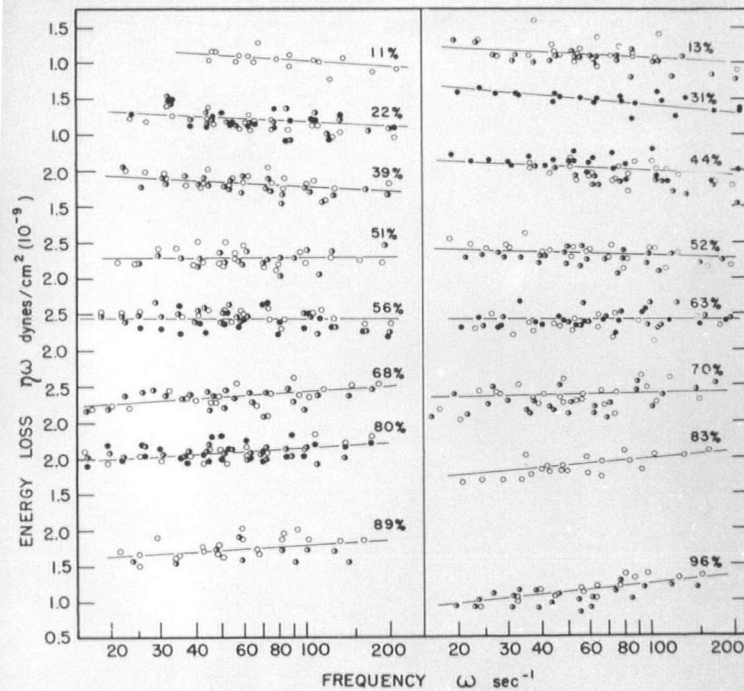


Figure 7. Energy loss  $E''$  as a function of log frequency at 35 °C. and various humidities.



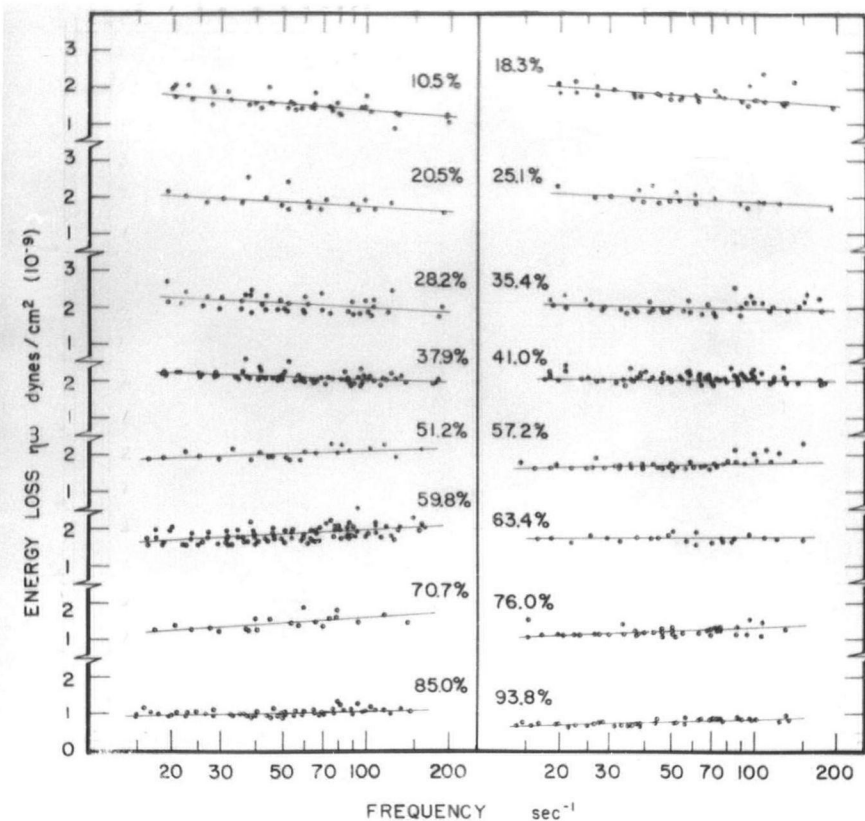


Figure 8. Energy loss  $E''$  as a function of log frequency at 60 °C. and various humidities.

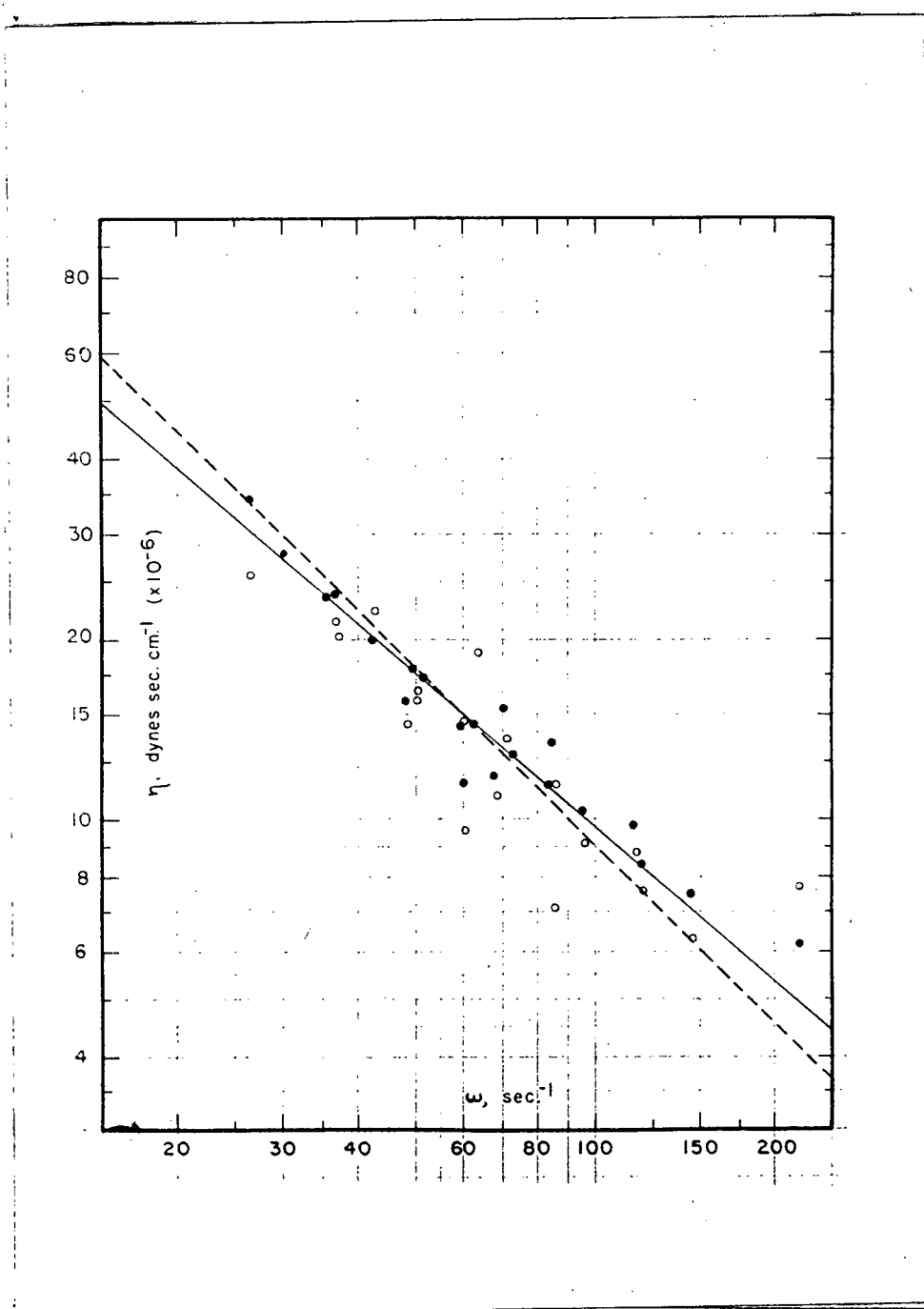


Figure 9.  $\log \eta$  as a function of  $\log \omega$  at 9 °C. and 9.5 % r.h., or 0.94 % water sorption.

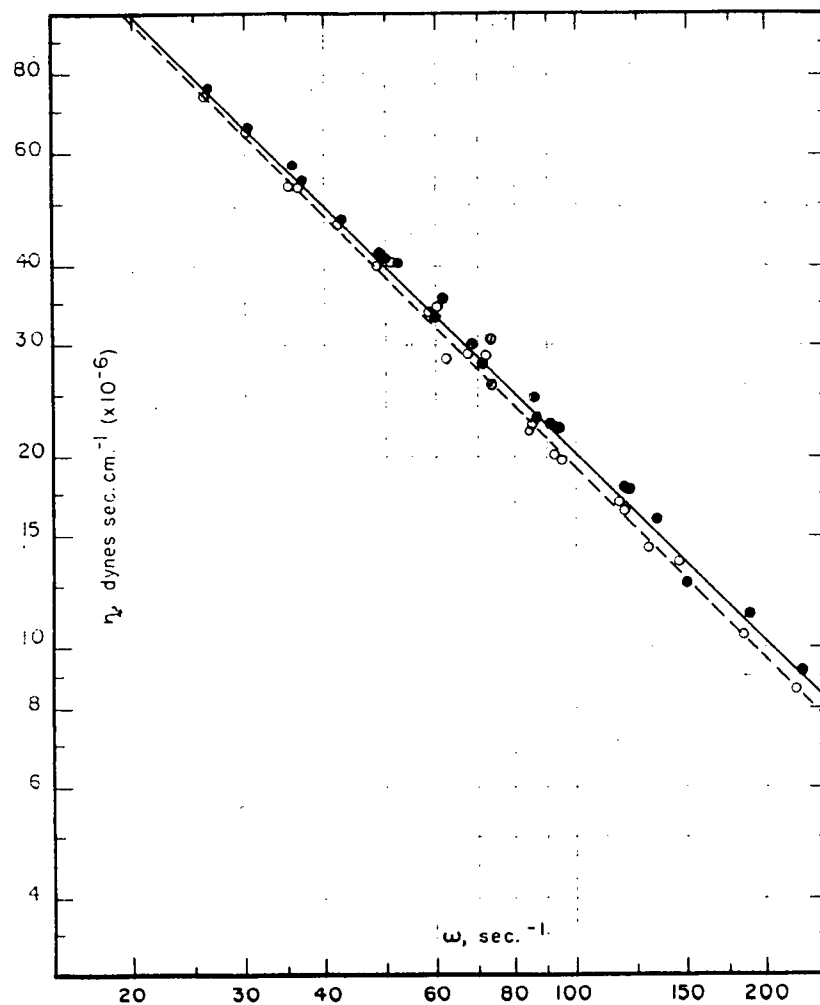


Figure 10.  $\log \eta$  as a function of  $\log \omega$  at 9 °C. and 48.2 % r.h., or 3.3 % water sorption.

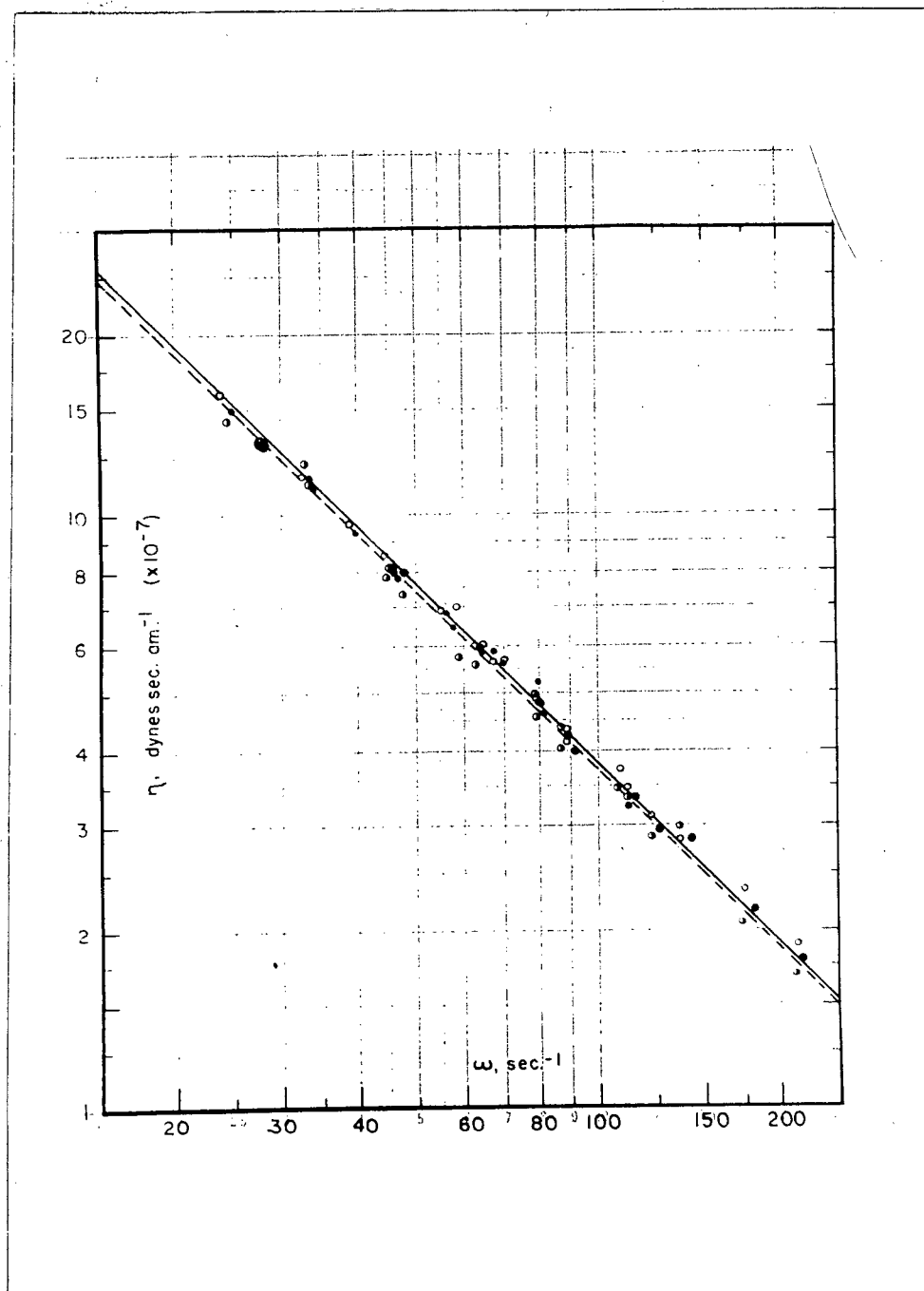


Figure 11.  $\log \eta$  as a function of  $\log \omega$  at 9 °C. and 76.0 percent r.h., or 5.35 % water sorption.

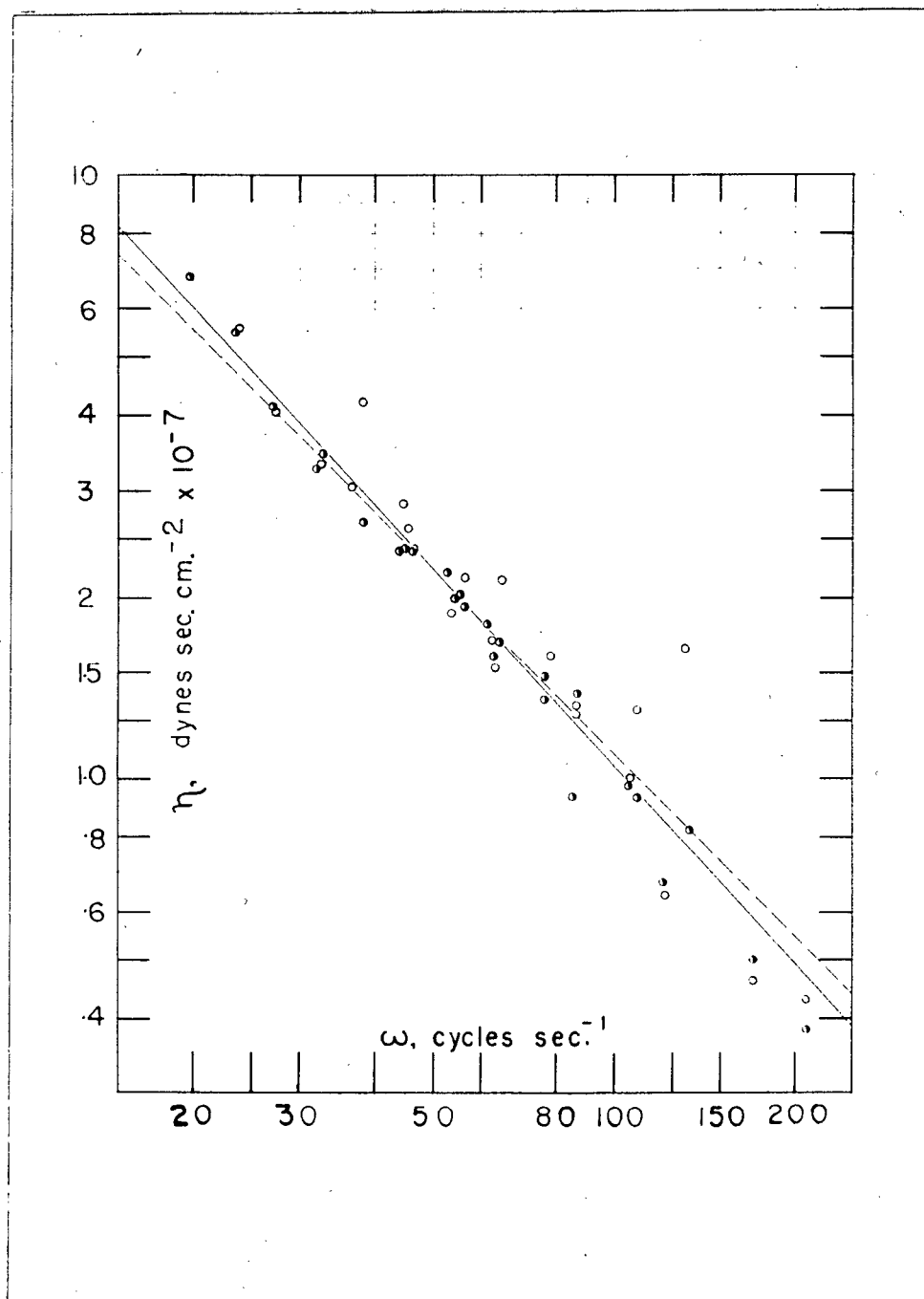


Figure 12.  $\log \eta$  as a function of  $\log \omega$  at 35 °C. and 13.8 percent r.h., or 0.92 % water sorption.

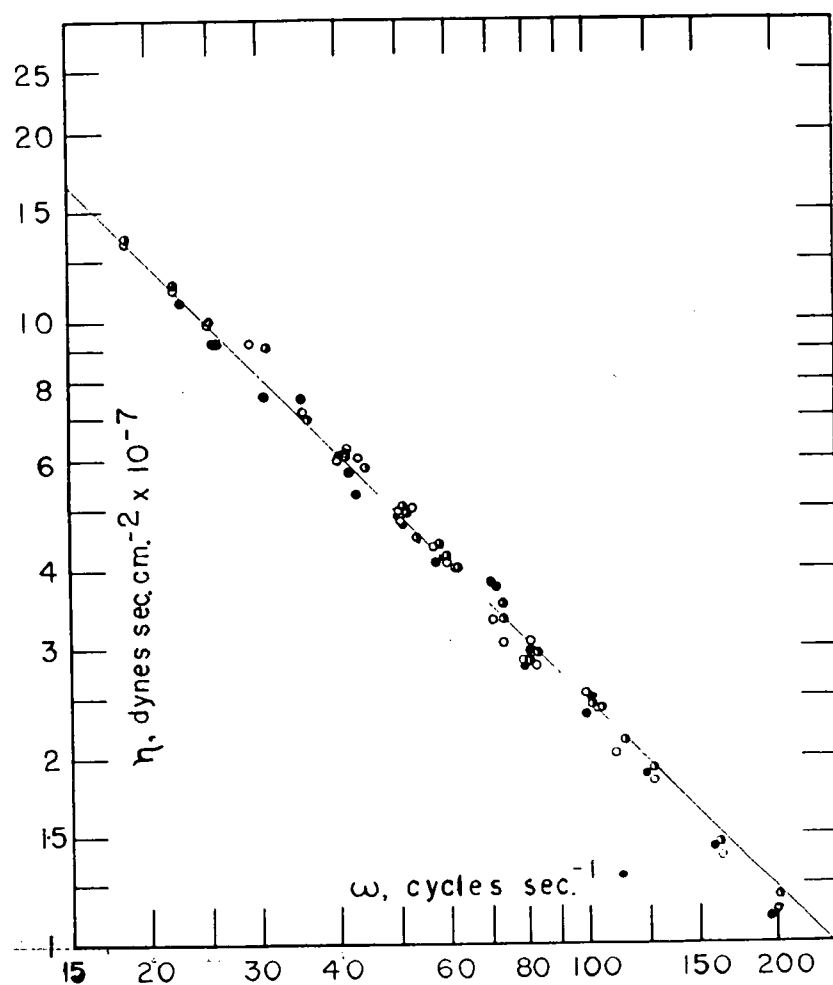


Figure 13. Log  $\eta$  as a function of log  $\omega$  at 35 °C. and 56.2 % r.h., or 3.25 % water sorption.

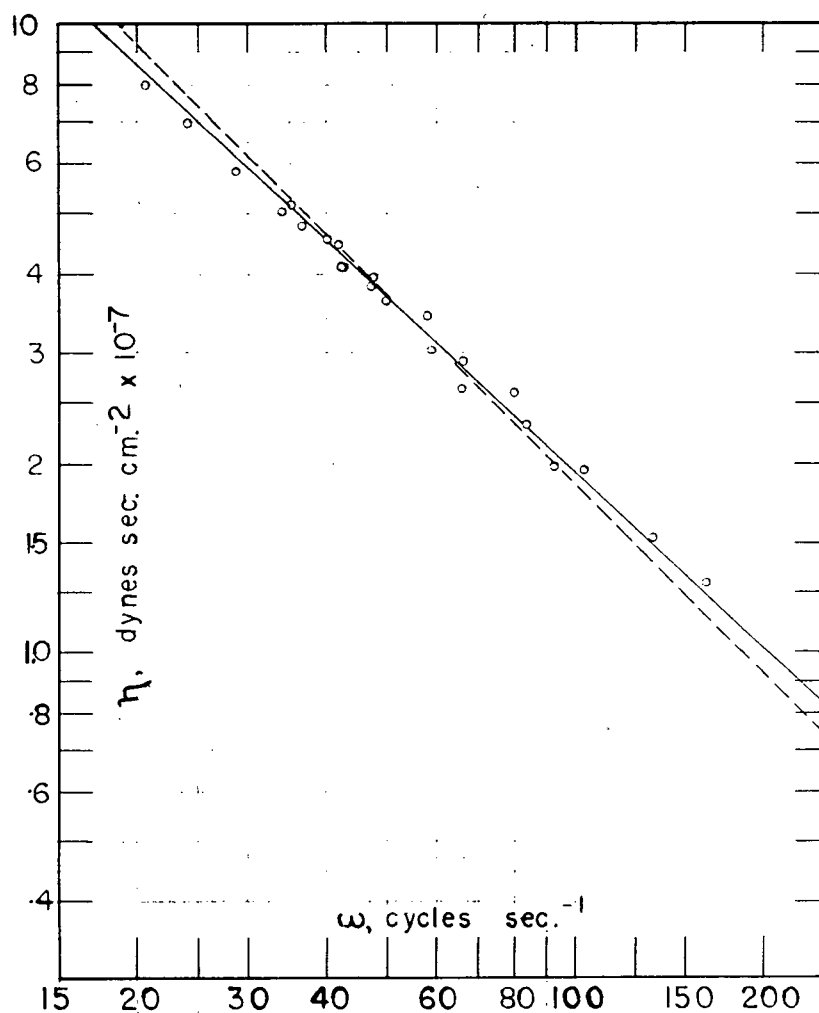


Figure 14.. Log  $\eta$  as a function of log circular frequency at 35 °C. and 82.7 % r.h., or 5.25 % water sorption.

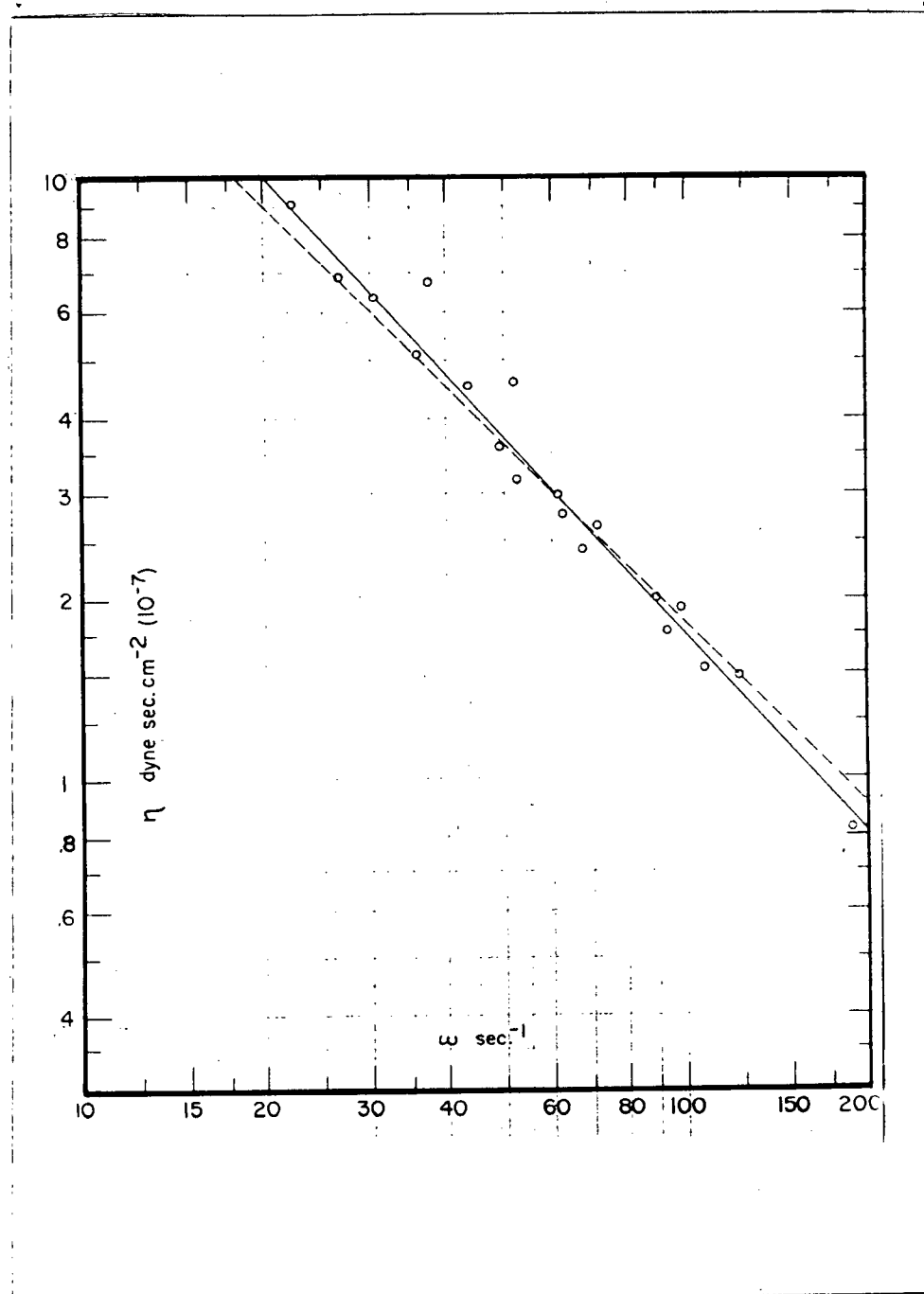


Figure 15. Log  $\eta$  as a function of log  $\omega$  at 60 °C. and 20.5 % r.h., or 0.95 % water sorption.



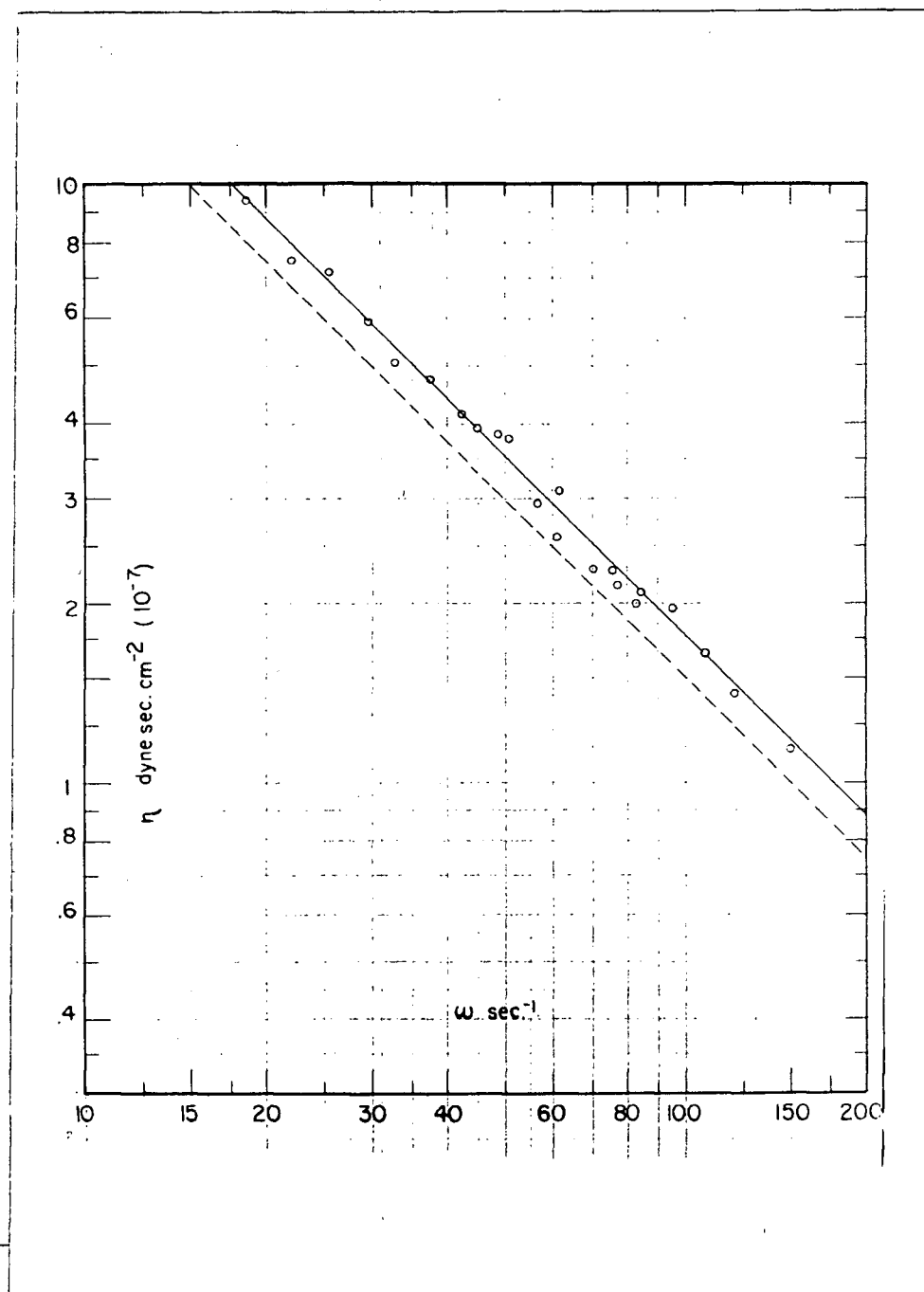


Figure 16. Log  $\eta$  as a function of log  $\omega$  at 60 °C. and 63.4 % r.h., or 3,10 % water sorption.

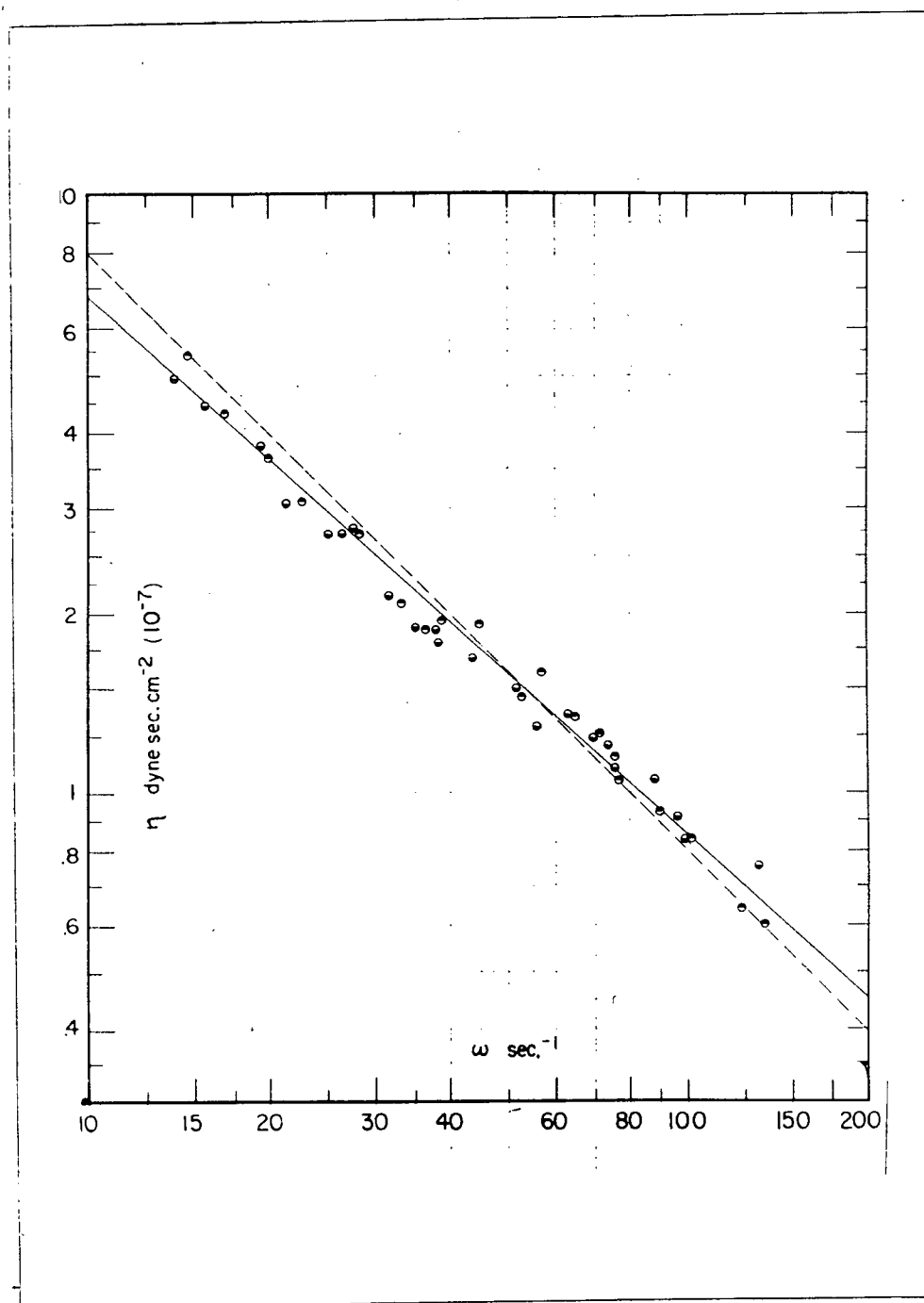


Figure 17.  $\log \eta$  as a function of  $\log \omega$  at 60 °C. and 93.8 % r.h., or 5.45 % water sorption.

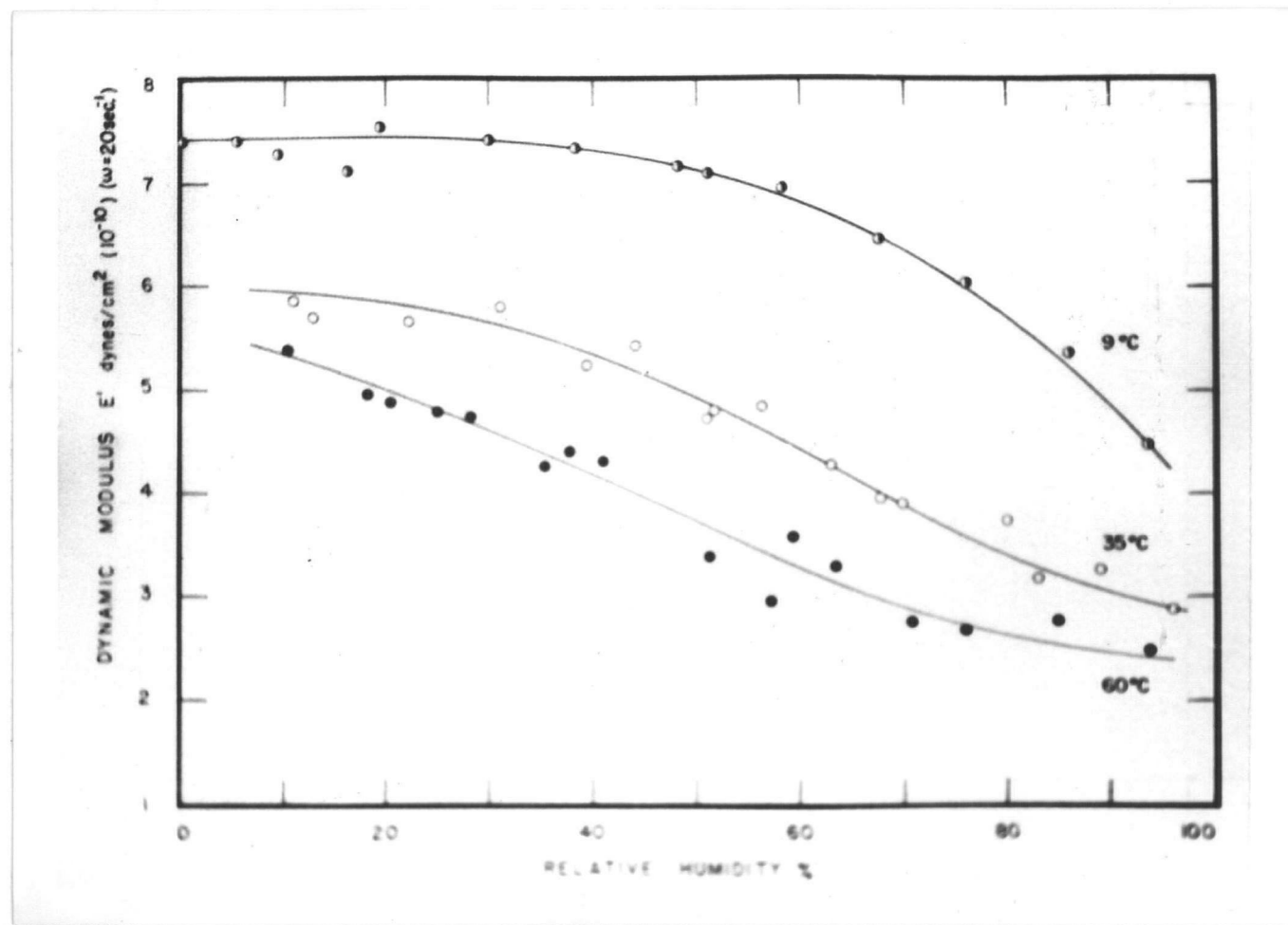


Figure 18. Dynamic modulus  $E'$  evaluated at  $\omega=20$  plotted against relative humidity.

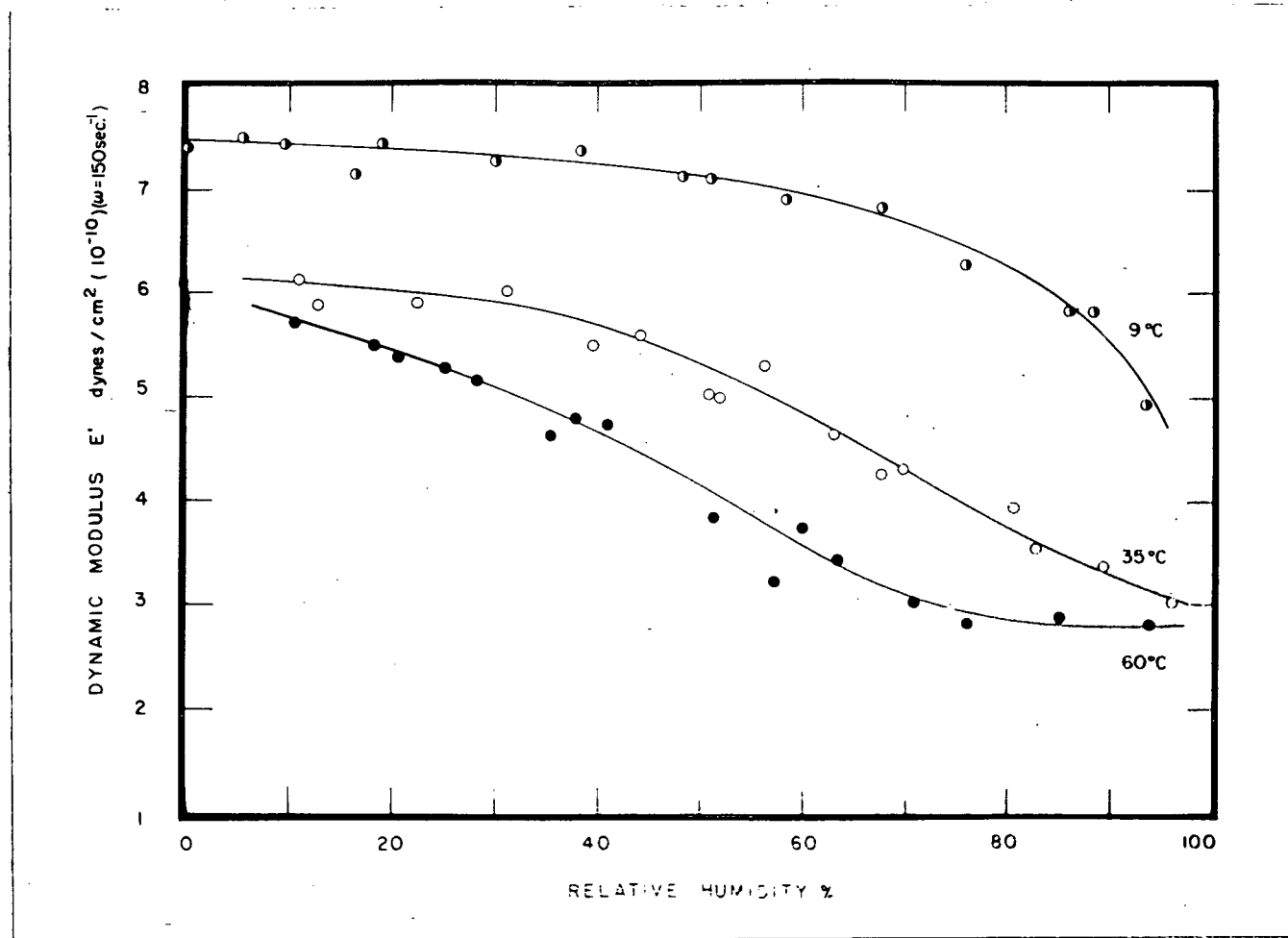


Figure 19. Dynamic modulus  $E'$  evaluated at  $\omega = 150$  plotted against relative humidity.

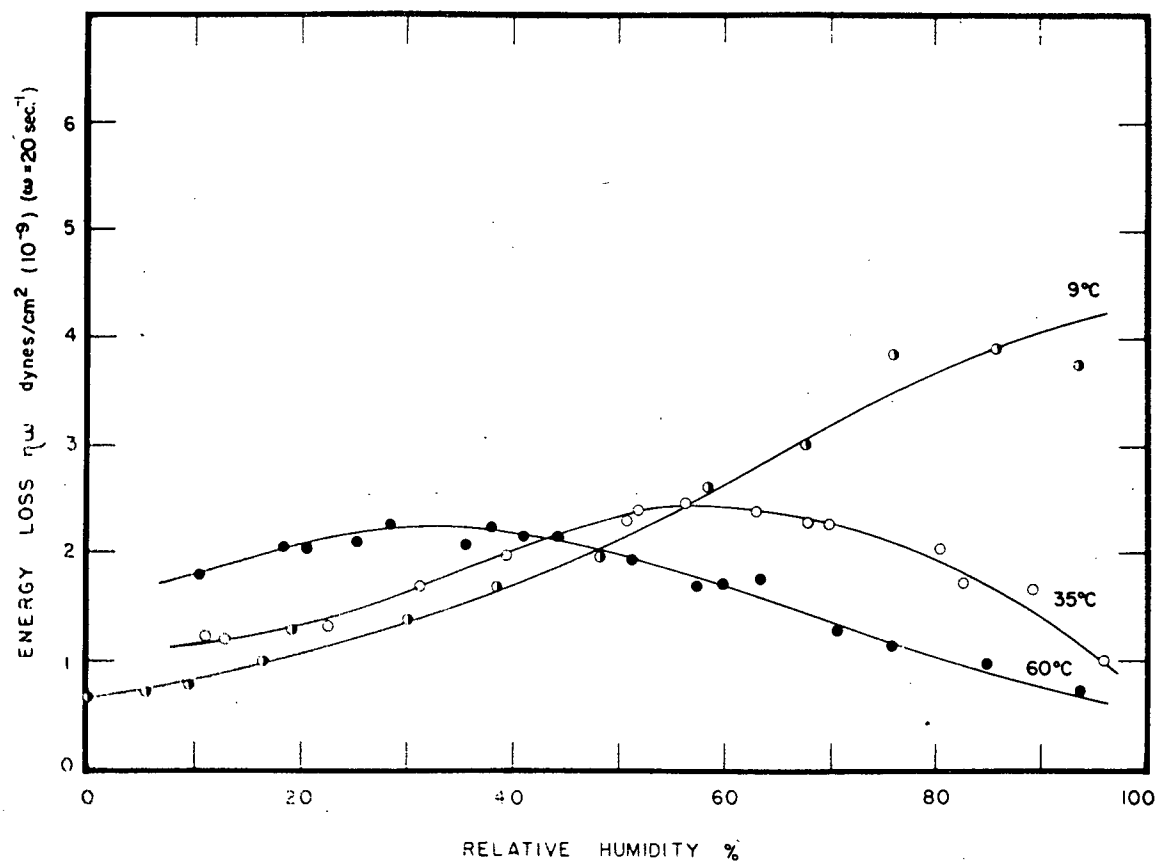


Figure 20. Energy loss  $E^h$  evaluated at  $\omega=20$  and plotted against relative humidity.

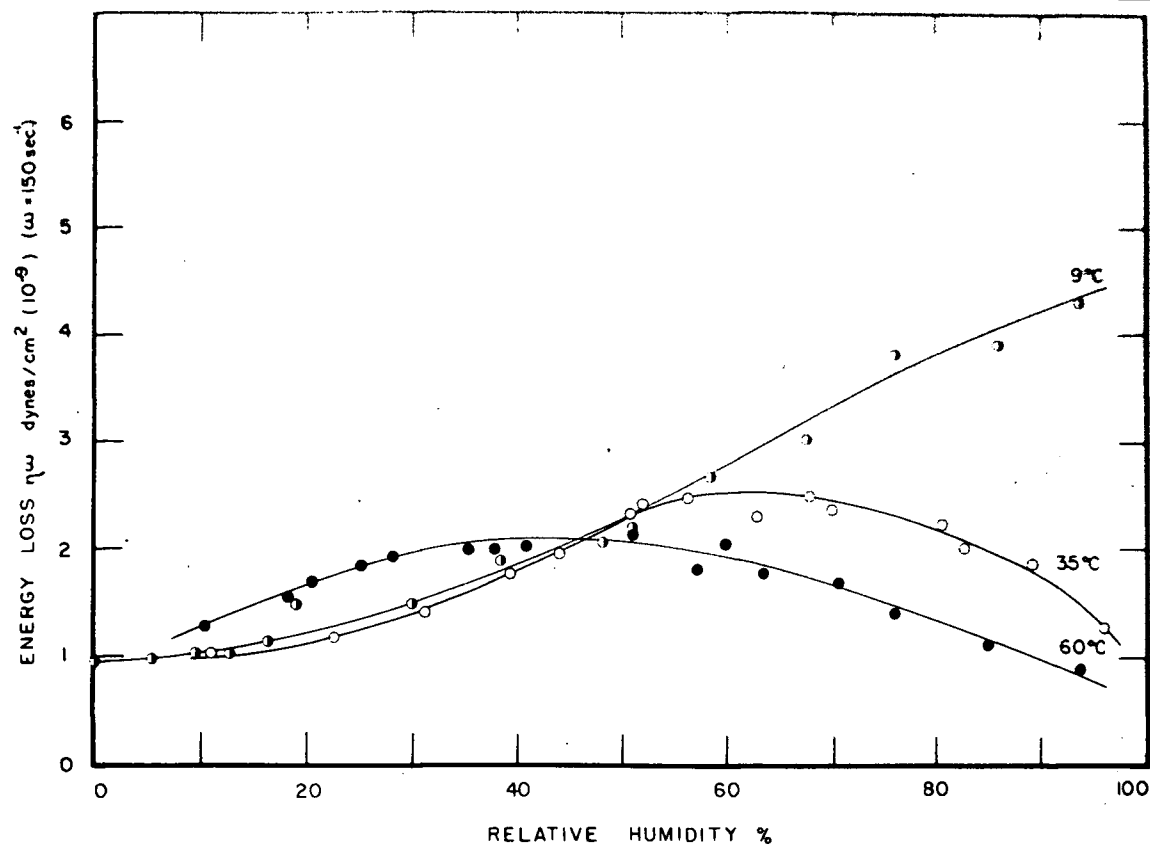


Figure 21. Energy loss  $E''$  evaluated at  $\omega = 150$  plotted against relative humidity.

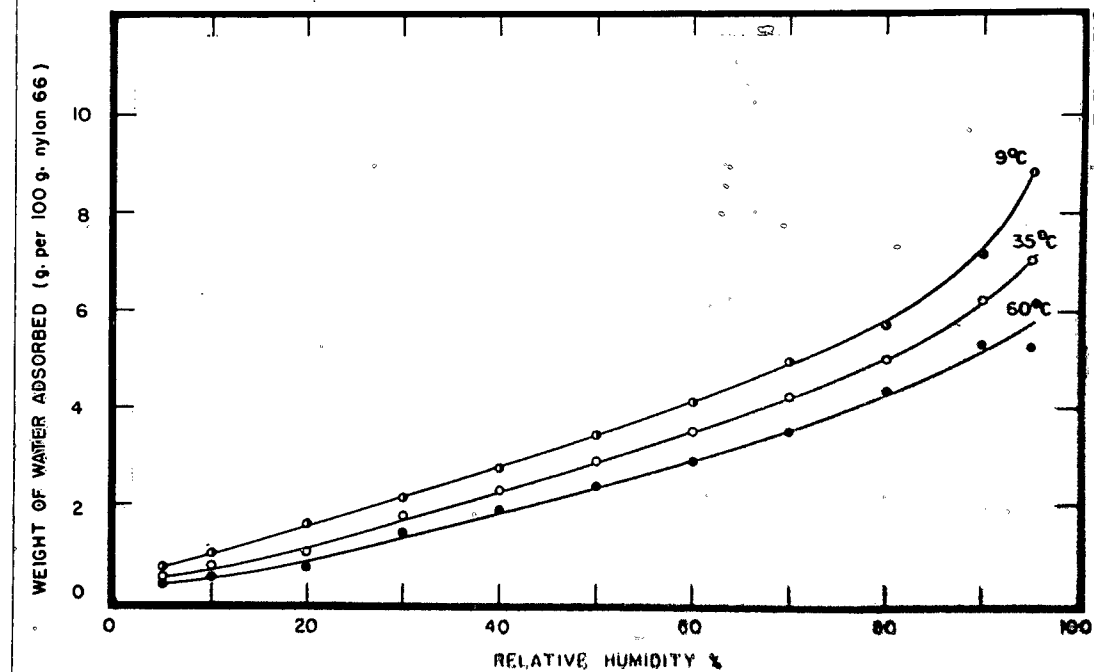


Figure 22. Weight percent of water sorbed by 100 g. of stretched nylon, at 9, 35, and 60 °C. The data are taken by extrapolation from Bull' results.

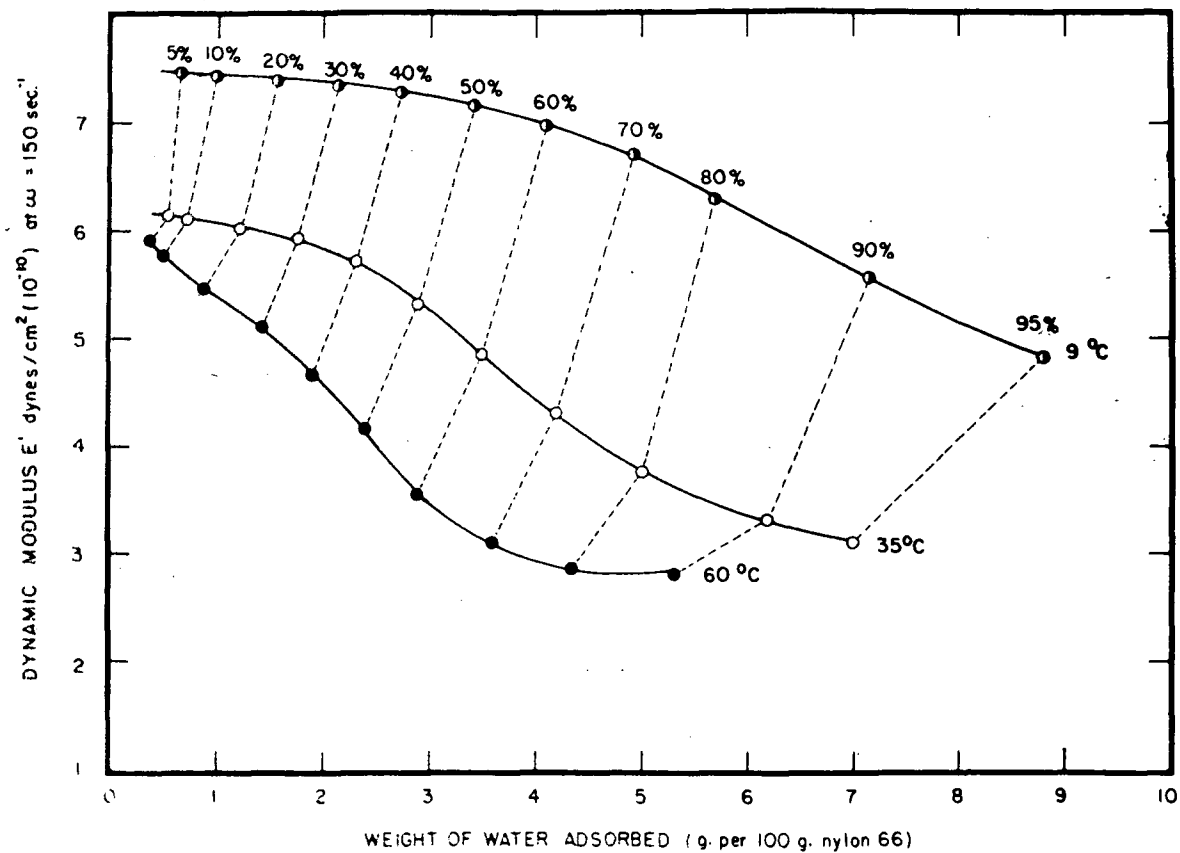


Figure 23. Dynamic modulus  $E'$ , evaluated at  $\omega = 150$  plotted against the weight of water adsorbed per 100 g. nylon.



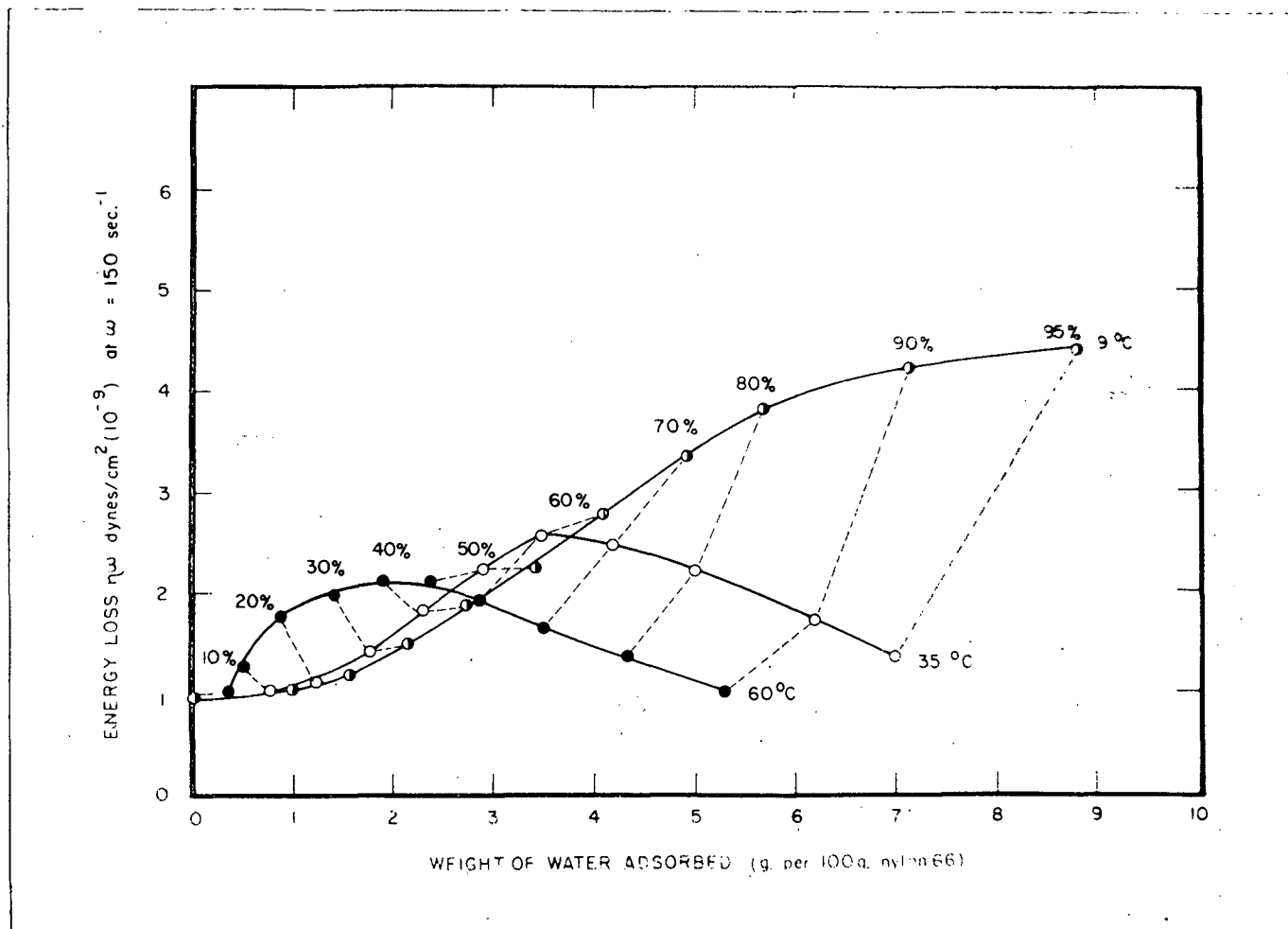


Figure 24. Energy loss  $E''$ , evaluated at  $\omega=150$ , plotted against the weight of water sorbed by 100 g. nylon.

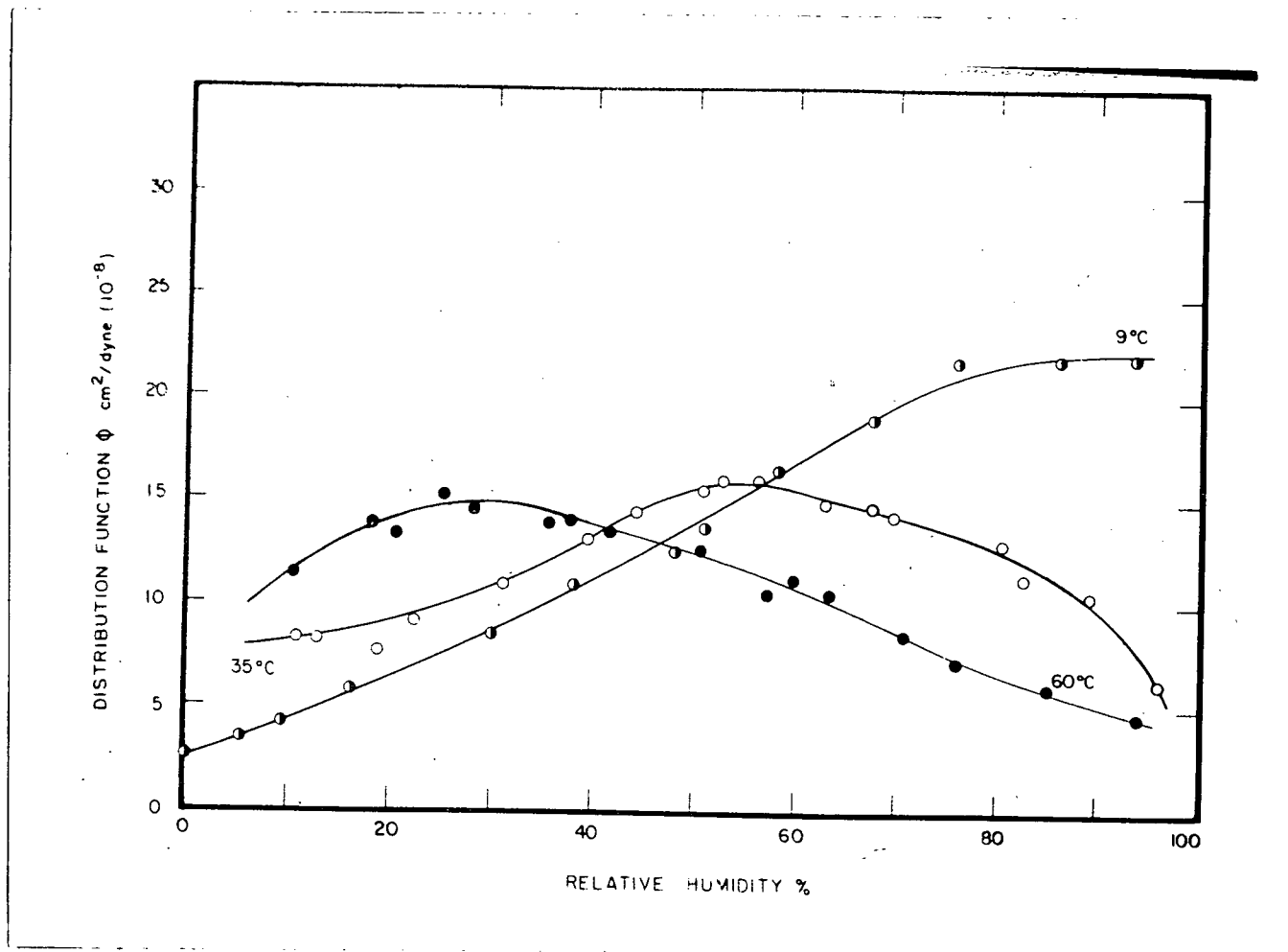


Figure 25. Distribution function  $\phi$ , evaluated at  $\omega=150$ , plotted against relative humidity.

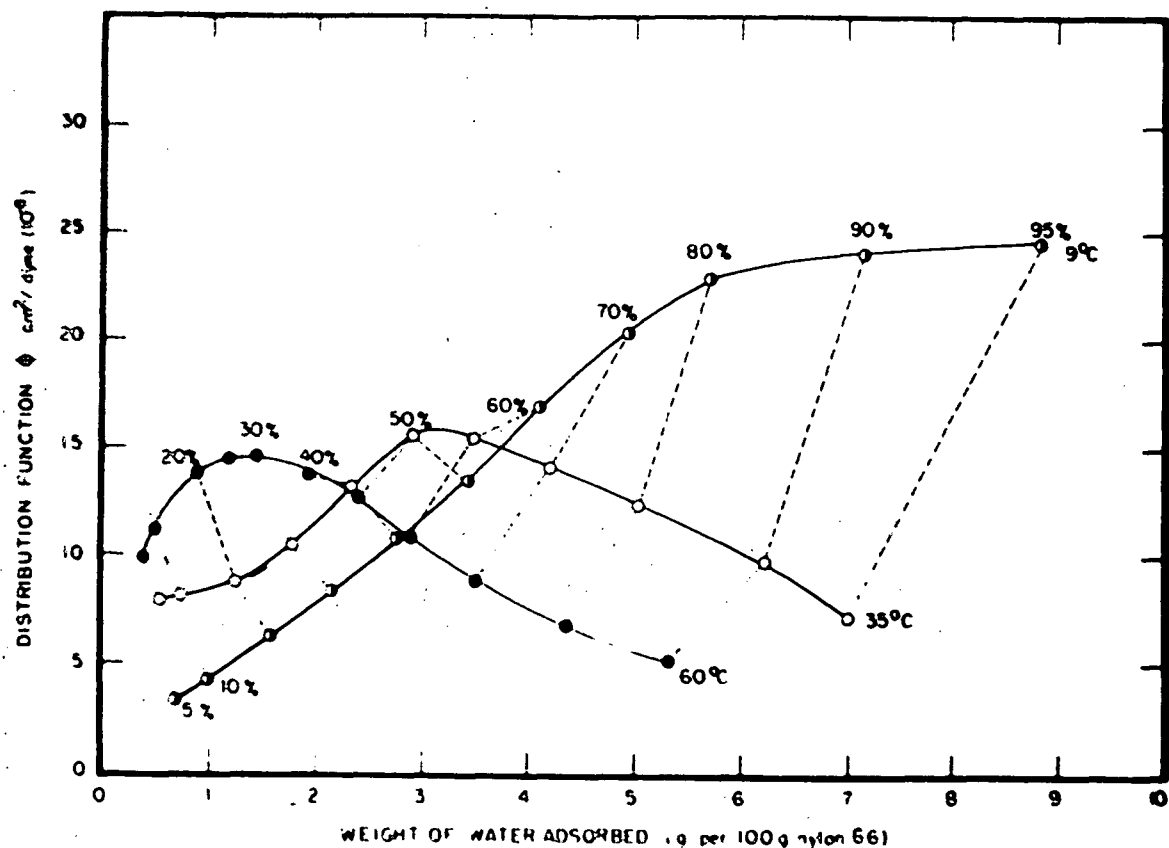


Figure 26. Distribution function  $\Phi$ , evaluated at  $\omega=150$  plotted against the weight of water sorbed by 100 g. nylon.